Supporting Information

Evaluation of the Potential of Single Particle ICP-MS for the Accurate Measurement of Number Concentration of AuNPs of Different Sizes and Coatings

Antonio R. Montoro Bustos[1]*, Karen E. Murphy[1], Michael R. Winchester[1]

[1]Chemical Sciences Division, Material Measurement Laboratory, National Institute of Standards and Technology, 100 Bureau Drive, Gaithersburg, MD 20899-1070.

Corresponding Author
* E-mail: antonio.montorobustos@nist.gov

ABSTRACT: Figures and additional information on the properties of commercial AuNPs, ICP-MS settings for single particle analysis, determination of transport efficiency, analytical performance of spICP-MS for the determination of PNC, total Au mass fraction, comparison between PNC_{direct} and various derived PNC for commercial AuNPs, computation of uncertainty budget for PNC determination and for the ratio between PNC_{direct} and derived *PNCs*.

Table of Contents

Calibration of spICP-MS for NP size determination

For the size determination of AuNP samples, a response factor, expressed in counts per ng of Au, was established from the signal intensities measured for RM 8013, used as a calibration standard.[1] In addition, RM 8013 is a well-suited calibration standard for sizing purposes because its particle mass falls in the middle of the range of masses of the materials analyzed in this study, which minimizes potential nonlinear responses. Assuming that AuNPs are spherical, solid, and have the density of bulk gold, and the various samples exhibit a similar response in the plasma to RM 8013, the corresponding mass of each particle event was calculated *via* the measured response factor and converted to particle size by eq S1:

$$d_{NP\,unk} = \left(\frac{I_{NP\,unk} - I_{diss\,unk} - I_{blk}}{I_{NP\,RM} - I_{diss\,RM} - I_{blk}}\right)^{\frac{1}{3}} \times\ d_{NP\,\mathrm{RM}} \times Rep \quad \text{(S1)}$$

where $d_{NP\,unk}$ (nm) is the diameter of the particle in the sample, $d_{NP\,RM}$ (nm) is the diameter of the particle in the standard, $I_{NP\,unk}$ and $I_{NP\,RM}$ (counts) are the intensity of the particle events for the sample and for the standard, respectively, $I_{diss\,unk}$ and $I_{diss\,RM}$ (counts) are the intensity of the dissolved background for the sample and for the standard, respectively (note that $I_{diss} = I_{background} - I_{blnk}$ where $I_{background}$ is all signal not identified as a particle event), I_{blk} (counts) is the intensity for the water blank, and *Rep* is the repeatability factor that represents the within laboratory repeatability of spICP-MS measurements, defined as the standard error of the measurements for *n* independent experiments.[1] In this project, the repeatability factor represents the variability of PNC_{direct} for the analysis of RM 8012 across 15 independent experiments conducted more than four years apart. *Rep* is expressed as a relative standard error and so is unitless. It is incorporated into eq S1 and S3 as a component with a value, x_i of 1 and $u(x_i)$ = (s/sqrt(n))/mean*100). Note that for the determination of the particle size and PNC of RM 8013, RM 8012 was used as a calibration standard. In this case, the consensus value for particle size derived from seven different single particle and ensemble sizing techniques listed in the NIST Reports of Investigation (ROIs)[2,3] applied to either RM 8013 or RM 8012, computed using the NIST "Consensus Builder" (https://consensus.nist.gov)[4,5], were used as particle diameters ($d_{NP\ RM}$) for calibration purposes. This consensus value was 55.6 nm, with an associated standard uncertainty of 0.25 nm for RM 8013, and 26.8 nm, with associated standard uncertainty of 0.51 nm for RM 8012.

Transport efficiency determination

The transport efficiency, defined as the ratio of the amount of analyte entering the plasma to the amount aspirated, is a crucial parameter for the correct particle size and number determination in spICP-MS. Transport efficiency was determined daily using freshly diluted AuNP suspensions of NIST RM 8013 *via* particle frequency method,[6] which is denoted as η_n. The η_n calculates the ratio of the number of detected particles to the theoretical number of particles delivered to the ICP-MS by eq S2:

$$\eta_n = \frac{N_{NP\ RM}}{q_{liq} \times t_{aq} \times PNC_{RM}} \quad \text{(S2)}$$

where η_n is the transport efficiency, $N_{NP\ RM}$ is the number of observed particle events for the calibration standard, q_{liq} (g min^{-1}) is the sample uptake rate, t_{aq} (min) is the time of acquisition, and PNC_{RM} (L^{-1}) is the derived particle number concentration of the gravimetrically diluted calibration standard suspension using eq 3.

Uncertainty Analysis for the determination of *PNC_{direct}*

For purposes of computing the combined uncertainty of PNC_{direct}, eq S2 and eq 3 were substituted into eq 2 to form the final measurement equation for the spICP-MS measurement of PNC_{direct}:

$$PNC_{direct} = \frac{N_{NP} \times 6 \times C_{S\,RM} \times q_{liq\,RM} \times t_{aq\,RM}}{N_{NP\,RM} \times q_{liq} \times t_{aq} \times 1E^{-18} \times d_{NP\,RM}{}^{3} \times Dil.F_{RM} \times \pi \times \rho} \times Dil.F \times Rep \quad (S3)$$

where PNC_{direct} (L^{-1}) is the target particle number concentration of the sample in the working suspension, N_{NP} and $N_{NP\,RM}$ are the number of observed particle events for the sample and for the standard, Cs is the Au mass fraction of the standard (μg·g^{-1}), q_{liq} and $q_{liq\,RM}$ (g min^{-1}) are the sample uptake rates for the sample and for the standard, t_{aq} and $t_{aq\,RM}$ (min) are the times of acquisition for the sample and the standard, $d_{NP\,RM}$ (nm) is the diameter of the particle in the standard, π is pi, ρ is the density of the particle (g·cm^{-3}), and $Dil.F$ and $Dil.F_{RM}$ are the dilution factors of stock suspension for the sample and for the standard. *Rep* is the repeatability factor that represents the variability of spICP-MS, defined as the standard error of the measurements for *n* independent experiments. Incomplete ionization of Au in the ICP was not included as a source of uncertainty because a similar behavior between the calibration standard and samples, analyzed under the same experimental conditions, was assumed.

Determination of Au mass fraction by conventional ICP-MS.

A Thermo Electron X Series X7 quadrupole ICP-MS was used for ICP-MS measurements. Samples were introduced into the ICP torch using a Quartz C-type nebulizer and impact bead spray chamber cooled to 2 °C. SRM 3140 Platinum Standard Solution and SRM 3124a Indium Standard Solution were used as internal standards for the determination of the total Au mass fraction. Total gold mass fraction was determined in triplicate after digestion of 0.5 g of the AuNP stock suspensions with a mixture of 0.15 mL of nitric and 1.5 mL of hydrochloric acids. After 1 hour, the mixtures were diluted with 45 mL of an internal standard solution containing Pt and In each at 1 ng g^{-1} in 1.5 % HNO_3. Subsequently, 0.063 mL of the diluted samples were added to 14 mL of the internal standard solution. Ionic Au calibration standards were prepared by serial dilution to range in mass fraction from 0.1 ng g^{-1} to 5 ng g^{-1} Au (n=6) using the internal standard solution. Procedural blanks (0.5 g of ultrapure water, n=10), calibration standards and sample digestions were analyzed by ICP-MS using a 0.45 mL min^{-1} sample flow rate and continuous data acquisition. Signal intensities at mass to charge (m/z) 115, 195, and 197 were measured at 10 ms dwell time per isotope. Three blocks of data, each 60 s in duration, were acquired per sample, and the mean intensities were used for computations.

Analytical performance of spICP-MS for the determination of PNC for NIST RM 8012 and RM 8013: linearity, limit of detection and precision of multiple-point calibration, and comparability with analyte transport efficiency determination

In spICP-MS analysis, very dilute suspensions of NPs are introduced into the ICP-MS instrument, such that statistically only one NP at a time enters the plasma. In these conditions, NP information appears as signal spikes superimposed on the steady state signal of the dissolved analyte. The fundamental assumption behind spICP-MS theory is that each pulse represents a single particle event.[7] Thus, the number of events counted is proportional to PNC (eq 2), which is only valid for low number concentrations that guarantee the detection of one NP per reading. The use of high number concentrations introduces a bias from the linear relationship between the number of events and PNC as a consequence of an increase of the probability of particle coincidence.[8]

The relationship between the number of events experimentally obtained by spICP-MS and the expected PNC concentration derived using the Au concentration and consensus particle size from ROI[2,3] was initially assessed using a multiple-point calibration for both NIST RM AuNPs with 7 different concentration levels (Figure S-1). Expected PNC concentration ranged over almost two orders of magnitude, from 5×10^5 L^{-1} to 3.5×10^7 L^{-1}. Calibration using RM 8013 resulted in a slightly steeper slope (dotted line, $m_{RM\ 8013} = 4.80 \times 10^{-5} \pm 0.10 \times 10^{-5}$ events L, $R^2 = 0.9979$) and a slightly better coefficient of determination compared to calibration using

RM 8012 (dashed line, $m_{RM\ 8012}$ = 4.59 x 10^{-5} ± 0.13 x 10^{-5} events L, R^2 = 0.9959). The difference of the slopes was 4.3 %, which indicates similar behavior of both NIST RM suspensions at the measured PNC levels. In fact, slopes of the calibration plots obtained from both NIST RMs were statistically similar, which confirms that the linear relationship between the number of events and expected PNC is independent of the particle diameter. The agreement between the slopes also indicate that the Au mass fraction and consensus particle diameter of each material, used to compute the derived PNC, reliably represent these two paramaters. Overall, linearity between the number of events and the expected PNC was confirmed across the range of concentrations of the working suspensions. Besides high homogeneity, high stability, and the negligible presence of unbound Au,[2,3] the good linearity achieved also shows the absence of coincident particle events.

The counting of NP events can be assimilated to an ideal Poisson counting process with zero blank, whose signal detection limit, based on the Currie Poisson-Normal approximation,[9] is associated with the capability of counting three NP events when no NP events are detected in a well-known procedural blank.[8] Thus, considering the slopes of the calibration plots, listed above, a limit of detection for PNC of 6.5 x 10^4 L^{-1} was obtained under the experimental conditions used in this work. This value is very similar to others reported in the literature when the time of analysis is adjusted.[10,11]

Precision of the PNC determination depends on the number of events counted. Using the acquisition conditions indicated in the Instrumentation section, relative standard deviations of 1.5% (n = 9) were obtained for RM 8013 at 1.5 × 10^7 L^{-1}, which entailed counting a total of 8500 events.

The most popular approach used in the literature for the determination of PNC by spICP-MS relies on the calculation of the analyte transport efficiency (eq S1). Between the different methods available for the calculation of transport efficiency, such as the particle size,[6] and the recently introduced dynamic mass flow approach,[12] the particle frequency method has been more extensively applied for the determination of PNC.[6] The last one is generally preferred over multi-point calibration, typically used to evaluate the linear relationship between the number of events and the number concentration, because it is a simplified version of the former that can be considered as a calibration with just one standard without compromising the uncertainty associated with the results.[8] For the evaluation of the capabilities of one-point calibration, a PNC of 1.5×10^7 L^{-1} from Figure S-1 was selected considering excellent precision and sufficient counting statistics. In case of RM 8013, the proportionality (or response) factor of the number of events and PNC for one-point calibration only differed by 0.60 % from the slope of the multiple-point calibration. This excellent agreement suggests that the selection of multiple-point or one-point calibration is not critical to achieve accurate determinations of PNC, provided NP standards and samples are diluted to an appropriate PNC to avoid coincident events. Note that to be sure that accurate results are obtained for unknown samples with a single point calibration requires a priori information on the number concentration or multiple runs until the proper dilution is achieved. This finding also justifies that, for the rest of the experiments, the quantification of PNC was carried out based on the more straightforward determination of the analyte transport efficiency (eq S1) and application of eq 2.

The long-term intermediate precision of the determination of transport efficiency using the frequency-based method was assessed for the analysis of RM 8012 and RM 8013 at a nominal PNC of 1.5×10^7 L^{-1} in fifteen separate experiments conducted more than four years apart using the same sample introduction system. Transport efficiency values of 1.94 ± 0.04 % and 1.85 ± 0.05 % were obtained using RM 8013, and RM 8012, respectively. Thus, measures of transport efficiency and for the estimated expanded uncertainty, *U*, at the 95 % coverage interval (95% C.I., < 3 % relative) yielded statistically similar results for both NIST RMs under long-term intermediate precision conditions,[13] which rules out any size dependent changes in transport efficiency[14] as well as degradation of the stock suspensions for these particular materials. The average probability of particle coincidence among the number of particle events, estimated by Poisson statistics,[15] was 1.1 % under the experimental conditions, which is considered appropriate to enable an accurate determination of PNC.

Considering the linear range, excellent long-term intermediate precision, together with an effective mitigation of undesired particle coincidence while maintaining adequate particle flow, a nominal PNC of 1.5×10^{7} L^{-1} was selected as the target concentration for the working suspensions of AuNP RM 8013, for the determination of the transport efficiency, as well as for all AuNP materials for the remainder of this study.

TABLES

Table S-1. Properties of gold nanoparticles (AuNPs) analyzed in this study.

AuNPs	Diameter (TEM), nm[a]	Hydrodynamic Diameter, nm	Au Mass Fraction, mg L^{-1}	pH of solution	Particle Surface	Solvent
NIST RM 8012, 30 nm	27.6 ± 2.1[b]	28.6 ± 0.9[c]	0.048	7.0	Sodium Citrate	Milli-Q Water
NIST RM 8013, 60 nm	56.0 ± 0.5[b]	56.6 ± 1.4[c]	0.052	7.3	Sodium Citrate	Milli-Q Water
30 nm PVP	29.7 ± 2.6	44.2	0.050	8.7	PVP	Milli-Q Water
30 nm bPEI	30.9 ± 2.9	27.0	0.052	8.9	bPEI	Milli-Q Water
30 nm PEG	32.7 ± 11.0	61.4	0.051	6.1	mPEG 5 kDa	Milli-Q Water
60 nm PVP	55.9 ± 7.9	92.3	0.054	5.9	PVP	Milli-Q Water
60 nm bPEI first lot	63.7 ± 7.3	79.1	0.052	8.9	bPEI	Milli-Q Water
60 nm bPEI second lot	61.0 ± 6.1	74.6	0.053	7.7	bPEI	Milli-Q Water
60 nm PEG first lot	65.3 ± 12.3	96.5	0.053	6.0	mPEG 5 kDa	Milli-Q Water
60 nm PEG second lot	64.1 ± 6.9	71.7	0.050	5.8	mPEG 5 kDa	Milli-Q Water
100 nm Citrate	104.0 ± 13.1	108.0	0.052	8.1	Sodium Citrate	Aqueous 2mM Citrate
100 nm PVP	100.0 ± 7.4	130.0	0.052	5.9	PVP	Milli-Q Water
100 nm bPEI	98.1 ± 10.1	108.5	0.052	8.7	bPEI	Milli-Q Water
100 nm PEG	104.7 ± 14.5	134.8	0.054	5.7	mPEG 5 kDa	Milli-Q Water

[a] Uncertainties correspond to one standard deviation, NPs analyzed n=100.

[b] Values indicate that the mean and uncertainties are the expanded uncertainty of the mean for 95% coverage, but only measurement repeatability was accounted for, NPs analyzed n=4364 for RM 8012 and 3030 for RM 8013.

[c] Expressed as Dynamic Light Scattering at 173° scattering angle (backscatter).

Table S-2. Instrument operating and data acquisition parameters for spICP-MS analysis

Instrument	Thermo Electron X Series X7 quadrupole ICP-MS
Sample introduction	Quartz C-type concentric nebulizer, cooled (2 °C) glass impact bead spray chamber
Type of Cones	High sensitivity (Xs) nickel sampler and skimmer
RF power (W)	1400
Plasma gas flow (L min^{-1})	13.0
Auxiliary gas flow (L min^{-1})	0.90
Nebulizer gas flow (L min^{-1})	0.86
Sampling depth (mm)	15
Nominal sample flow rate (mL min^{-1})	0.5
Dwell time (ms)	10
Acquisition time (s)	360

Table S-3. Comparison between mean particle diameter, expressed as Huber estimates of particle size location (or central tendency), by TEM (results provided by the supplier)[2,3,16] and results reported by HR-SEM[1] and spICP-MS[1] for NIST RM 8012 and 8013, and for different commercial AuNPs, respectively.

	TEM supplier	HR-SEM diameter	spICP-MS diameter
RM 8012 (nm)	27.0 ± 0.1	27.0 ± 0.1 (3.2) [a]	27.2 ± 0.1 (0.8) [a]
NPs analyzed	4364	14745	5055
MAD (nm)	1.9	1.8	2.0
RM 8013	55.5 ± 0.1	55.0 ± 0.1 (3.6) [a]	54.1 ± 0.1 (7.6) [a]
NPs analyzed	3030	3137	5964
MAD (nm)	3.3	3.0	3.4
30 nm PVP (nm)	29.8 ± 0.4	29.5 ± 0.1 (3.2) [a]	30.0 ± 0.1 (0.6) [a]
NPs analyzed	137	4811	2705
MAD (nm)	2.4	2.1	2.4
30 nm bPEI (nm)	30.8 ± 0.6	31.5 ± 0.1 (3.3) [a]	31.0 ± 0.2 (0.6) [a]
NPs analyzed	100	7255	1575
MAD (nm)	2.8	3.9	3.2
30 nm PEG (nm)	32.6 ± 0.6	29.9 ± 0.1 (3.2) [a]	30.6 ± 0.1 (0.7) [a]
NPs analyzed	125	3985	2743
MAD (nm)	3.2	3.2	3.0
60 nm PVP (nm)	56.3 ± 1.6	59.6 ± 0.2 (3.7) [a]	58.6 ± 0.4 (0.9) [a]
NPs analyzed	100	11515	1812
MAD (nm)	8.4	7.5	7.0
60 nm bPEI first lot (nm)	64.4 ± 1.5	60.3 ± 0.2 (3.7) [a]	60.2 ± 0.3 (1.1) [a]
NPs analyzed	100	3236	1706
MAD (nm)	6.8	6.5	6.4
60 nm bPEI second lot (nm)	61.6 ± 1.4	58.9 ± 0.2 (3.6) [a]	58.8 ± 0.3 (1.2) [a]
NPs analyzed	100	6290	3920
MAD (nm)	4.7	6.3	8.7
60 nm PEG first lot (nm)	65.5 ± 1.6	57.8 ± 0.3 (3.6) [a]	56.7 ± 0.3 (0.8) [a]

NPs analyzed	100	2538	2562
MAD (nm)	8.4	8.5	8.1
60 nm PEG second lot (nm)	64.6 ± 1.5	59.7 ± 0.2 (3.7) [a]	58.3 ± 0.3 (2.9) [a]
NPs analyzed	100	6279	3409
MAD (nm)	6.6	8.0	8.1
100 nm Citrate (nm)	105.0 ± 2.6	98.8 ± 0.3 (4.5) [a]	93.2 ± 0.6 (2.0) [a]
NPs analyzed	100	6303	2820
MAD (nm)	15.0	11.7	14.9
100 nm PVP (nm)	100.2 ± 1.4	95.5 ± 0.2 (4.4) [a]	95.5 ± 0.6 (3.5) [a]
NPs analyzed	100	7293	1921
MAD (nm)	8.4	8.1	11.4
100 nm bPEI (nm)	99.1 ± 2.2	95.8 ± 0.3 (4.4) [a]	94.4 ± 0.5 (2.5) [a]
NPs analyzed	102	5200	2982
MAD (nm)	6.9	7.5	11.6
100 nm PEG (nm)	105.5 ± 2.8	94.4 ± 0.4 (4.4) [a]	98.8 ± 0.6 (3.8) [a]
NPs analyzed	125	3007	2451
MAD (nm)	14.1	12.8	15.6

Values indicate the Huber estimates of particle-size location and the standard uncertainty associated with the Huber estimate.

[a] Expanded uncertainties associated with the spICP-MS and HR-SEM size determinations included a best estimate of known or suspected sources of bias were included in the parenthetical uncertainty computation.

Table S-4. Breakdown of uncertainty analysis for spICP-MS determination of *PNC_{direct}* for NIST RM 8012. Values for the input quantities correspond to a representative spICP-MS determination of *PNC_{direct}* of the fifteen experiments.

Source of uncertainty	Quantity Value	Standard Uncertainty	Description	Relative Contribution (%)
Particle size consensus value for standard ($d_{NP\ RM}$) (nm)	55.6	0.25 (B)	Estimated standard uncertainty from the seven ROI-reported diameter measurements for RM 8013[3]	4.3
Dilution Factor of stock suspension for the sample (*Dil.F*) (g)	7.45 x 10^6	6.51 x 10^4 (B)	Estimated standard uncertainty of the gravimetrically measured sample dilution factor	1.8
Measurement repeatability (*Rep*)	1	0.017 (A)	Relative standard error of the results for n = 15 experiments	6.7
Number of observed events for the sample (N_{NP})	551	27 (A)	Standard uncertainty of three replicate measurements of the number of particles	55.1
Au mass fraction of the standard (C_S) (µg g^{-1})	51.86	0.32 (A)	Combined standard uncertainty of the Au mass fraction measurement for RM 8013 from the ROI[3]	0.9
Sample uptake rate for the standard ($q_{liq\ RM}$) (g min^{-1})	0.582	0.00291 (A)	Standard uncertainty of three replicate measurements of the sample flow rate for RM 8013	0.6
Time of acquisition for the standard ($t_{aq\ RM}$) (min)	1.66	0.0002 (A)	Standard uncertainty of the analysis time for three replicates measurement of RM 8013	0.0
Number of observed events for the standard ($N_{NP\ RM}$)	522	19 (A)	Standard uncertainty of three replicate measurements of the number of particles for RM 8013	29.1
Sample uptake rate for the sample (q_{liq}) (g min^{-1})	0.582	0.00291 (A)	Standard uncertainty of three replicate measurements of the sample flow rate	0.6
Time of acquisition for the sample (t_{aq}) (min)	1.66	0.0002 (A)	Standard uncertainty of the analysis time for three replicates measurement of the sample	0.0
Dilution Factor of stock suspension for the standard ($Dil.F_{RM}$) (g)	1.05 x 10^6	7.23 x 10^3 (B)	Estimated standard uncertainty of the gravimetrically measured RM 8013 dilution factor	1.1
Density of the particles (ρ) (g cm^{-3})	19.30	0.01 (B)	Estimated standard uncertainty of the bulk density of Au[17]	0.0
MF Value, *PNC_{direct}* RM 8012 (L^{-1})	2.24 x 10^{14}			
Combined standard uncertainty, uc (L^{-1})	1.5 x 10^{13}			
Expanded k=2 uncertainty, U (L^{-1})	2.9 x 10^{13}			
% Relative Expanded, U_r	12.9 %			

(A) and (B) correspond to Type A and Type B methods used for the evaluation of uncertainty.

Table S-5. PNC values derived for NIST AuNP RMs based on the combination of Au mass fraction[2,3] with: (first column) the Huber estimates of particle size location (or central tendency), or (second column) the full particle size distribution reported by TEM (NIST ROI),[2,3] HR-SEM,[1] and spICP-MS.[1]

	Central Tendency (PNC_{mean})[a]	Full PSD ($PNC_{distribution}$)
RM 8012		
Reported diameter (ROI)	$2.48 \times 10^{14} \pm 0.28 \times 10^{14}$ L^{-1}	$2.63 \times 10^{14} \pm 0.31 \times 10^{14}$ L^{-1} [c]
HR-SEM[b]	$2.42 \times 10^{14} \pm 0.93 \times 10^{14}$ L^{-1}	$2.47 \times 10^{14} \pm 0.94 \times 10^{14}$ L^{-1}
spICP-MS[b]	$2.37 \times 10^{14} \pm 0.21 \times 10^{14}$ L^{-1}	$2.76 \times 10^{14} \pm 0.29 \times 10^{14}$ L^{-1}
RM 8013		
Reported diameter (ROI)	$2.99 \times 10^{13} \pm 0.09 \times 10^{13}$ L^{-1}	$3.10 \times 10^{13} \pm 0.13 \times 10^{13}$ L^{-1} [c]
HR-SEM[b]	$3.08 \times 10^{13} \pm 0.61 \times 10^{13}$ L^{-1}	$3.14 \times 10^{13} \pm 0.62 \times 10^{13}$ L^{-1}
spICP-MS[b]	$3.24 \times 10^{13} \pm 1.43 \times 10^{13}$ L^{-1}	$3.37 \times 10^{13} \pm 1.49 \times 10^{13}$ L^{-1}

[a] Assumes all analyte is present as spherical NPs of the central tendency diameter.

[b] Expanded uncertainties associated with the spICP-MS and HR-SEM size determinations included a best estimate of known or suspected sources of bias.[1]

[c] PNC derived from the full particle size distribution obtained by TEM (NIST Report of Investigation).[2,3]

Listed uncertainties are based on a confidence interval, with the coverage factor, k = 2 corresponding to approximately 95 % confidence.

Table S-6. Breakdown of uncertainty analysis associated with PNC_{mean} for RM 8012 derived based on the combination of Au mass fraction with the particle size consensus value,[2,3] and mean particle diameter reported by HR-SEM,[1] and spICP-MS.[1]

Report diameter (ROI):

Source of uncertainty	Quantity Value	Standard Uncertainty	Description	Relative contribution (%)
Au mass fraction of the material (C_S) (µg g^{-1})	48.17	0.17 (A)	Combined standard uncertainty of the Au mass fraction measurement for RM 8012 from the ROI[3]	0.4
Particle size for the material ($d_{NP\ RM}$) (nm)	26.8	0.51 (B)	Estimated standard uncertainty from the seven ROI-reported diameter measurements for RM 8012[3]	99.6
Density of the particles (ρ) (g cm^{-3})	19.30	0.01 (B)	Estimated standard uncertainty of the bulk density of Au[17]	0.0
MF Value, PNC_{mean} RM 8012 (L^{-1})	2.48 x 10^{14}			
Combined standard uncertainty (L^{-1})	1.4 x 10^{13}			
Expanded k=2 uncertainty (L^{-1})	2.8 x 10^{13}			
% Relative Expanded, U_r	11.3 %			

HR-SEM

Source of uncertainty	Quantity Value	Standard Uncertainty	Description	Relative contribution (%)
Au mass fraction of the material (C_S) (µg g^{-1})	48.17	0.17 (A)	Combined standard uncertainty of the Au mass fraction measurement for RM 8012 from the ROI[3]	0.1
Particle size for the material ($d_{NP\ RM}$) (nm)	27.0	1.62 (B)	Estimated standard uncertainty of the HR-SEM particle diameter reported for RM 8012[1]	99.9
Density of the particles (ρ) (g cm^{-3})	19.30	0.01 (B)	Estimated standard uncertainty of the bulk density of Au[17]	0.0
MF Value, PNC_{mean} RM 8012 (L^{-1})	2.42 x 10^{14}			
Combined standard uncertainty (L^{-1})	4.7 x 10^{13}			
Expanded k=2 uncertainty (L^{-1})	9.3 x 10^{13}			
% Relative Expanded, U_r	38.2 %			

spICP-MS				
Source of uncertainty	**Quantity Value**	**Standard Uncertainty**	**Description**	**Relative contribution (%)**
Au mass fraction of the material (C_S) (µg g^{-1})	48.17	0.17 (A)	Combined standard uncertainty of the Au mass fraction measurement for RM 8012 from the ROI[3]	0.7
Particle size for the material ($d_{NP\ RM}$) (nm)	27.2	0.4 (B)	Estimated standard uncertainty of the spICP-MS particle diameter reported for RM 8012[1]	99.3
Density of the particles (ρ) (g cm^{-3})	19.30	0.01 (B)	Estimated standard uncertainty of the bulk density of Au[17]	0.0
MF Value, PNC_{mean} RM 8012 (L^{-1})	2.37×10^{14}			
Combined standard uncertainty (L^{-1})	1.1×10^{13}			
Expanded k=2 uncertainty (L^{-1})	2.1×10^{13}			
% Relative Expanded, U_r	8.9 %			

(A) and (B) correspond to Type A and Type B methods used for the evaluation of uncertainty.

Table S-7. Uncertainty budget for the calculation of the derived PNC_{mean} of NIST RM 8012 and RM 8013. Consensus value derived from the seven measurement results listed in the NIST ROIs[2,3] (first column), and the Huber estimates of particle size (or central tendency) obtained by HR-SEM[1] (second column), and spICP-MS[1] (third column) for NIST AuNP RMs were combined with Au mass fraction[2,3] to derive PNC_{mean}.

For NIST RM 8012:	**Report diameter (ROI) (PNC_{mean} 2.48 x 10^{14} L^{-1})**	**HR-SEM (PNC_{mean} 2.42 x 10^{14} L^{-1})**	**spICP-MS (PNC_{mean} 2.37 x 10^{14} L^{-1})**
Source of uncertainty	**Relative contribution (%)**	**Relative contribution (%)**	**Relative contribution (%)**
Au mass fraction of the material (C_S)	0.4	< 0.0	0.6
Particle size for the material ($d_{NP\ RM}$)	99.3	96.9	99.2
Density of the particles (ρ)	< 0.0	< 0.0	< 0.0
Residual	0.3	3.2	0.3
Combined standard uncertainty (L^{-1})	1.4 x 10^{13} L^{-1}	4.7 x 10^{13} L^{-1}	1.1 x 10^{13} L^{-1}
Expanded k=2 uncertainty (L^{-1})	2.8 x 10^{13} L^{-1}	9.3 x 10^{13} L^{-1}	2.1 x 10^{13} L^{-1}

For NIST RM 8013:	**Report diameter (ROI) (PNC_{mean} 2.99 x 10^{13} L^{-1})**	**HR-SEM (PNC_{mean} 3.08 x $10^{13}$$L^{-1}$)**	**spICP-MS (PNC_{mean} 3.24 x $10^{13}$$L^{-1}$)**
Source of uncertainty	**Relative contribution (%)**	**Relative contribution (%)**	**Relative contribution (%)**
Au mass fraction of the material (C_S)	17.2	0.4	0.1
Particle size for the material ($d_{NP\ RM}$)	82.7	98.7	95.7
Density of the particles (ρ)	0.1	< 0.0	< 0.0
Residual	< 0.0	0.9	4.2
Combined standard uncertainty (L^{-1})	0.04 x 10^{13} L^{-1}	0.31 x 10^{13} L^{-1}	0.7 x 10^{13} L^{-1}
Expanded k=2 uncertainty (L^{-1})	0.09 x 10^{13} L^{-1}	0.61 x 10^{13} L^{-1}	1.4 x 10^{13} L^{-1}

Table S-8. Uncertainty budget for the ratio between PNC_{direct} obtained across 15 independent spICP-MS experiments, expressed in percentage, and PNC_{mean} for RM 8012 and RM 8013. PNC_{mean} values reported for purposes of comparison to PNC_{direct} were derived based on the combination of Au mass fraction[2,3] and: the consensus value derived from the seven measurement results listed in the NIST ROIs[2,3] (first column), and the Huber estimates of particle size (or central tendency) reported by HR-SEM[1] (second column), and spICP-MS[1] (third column).

For NIST RM 8012:	**Reported diameter (ROI) (PNC_{direct}/PNC_{mean}) 95.9 %**	**HR-SEM diameter (PNC_{direct}/PNC_{mean}) 98.4 %**	**spICP-MS diameter (PNC_{direct}/PNC_{mean}) 100.4 %**
Source of uncertainty	**Relative contribution (%)**	**Relative contribution (%)**	**Relative contribution (%)**
Particle size consensus value for standard ($d_{NP\ RM}$)	0.3	< 0.0	0.4
Dilution Factor of stock suspension for the sample (*Dil.F*)	0.1	< 0.0	0.2
Measurement repeatability (*Rep*)	0.4	< 0.0	0.7
Number of observed events for the sample (N_{NP})	3.6	0.3	5.6
Au mass fraction of the standard ($C_{S\ RM}$)	0.1	< 0.0	0.1
Sample uptake rate for the standard ($q_{liq\ RM}$)	0.1	< 0.0	0.1
Time of acquisition for the standard ($t_{aq\ RM}$)	< 0.0	< 0.0	< 0.0
Number of observed events for the standard ($N_{NP\ RM}$)	1.9	0.2	3.0
Sample uptake rate for the sample (q_{liq})	0.1	< 0.0	0.1
Time of acquisition for the sample (t_{aq})	< 0.0	< 0.0	< 0.0
Dilution Factor of stock suspension for the standard ($Dil.F_{RM}$)	1.1	< 0.0	0.1
Particle size for the sample (d_{NP})	92.8	96.3	89.0
Au mass fraction of the sample (C_S)	0.3	< 0.0	0.5
Density of the particles (ρ)	< 0.0	< 0.0	< 0.0
Residual	0.3	3.0	0.3
Combined standard uncertainty (%)	5.7 %	19.3 %	4.7 %
Expanded k=2 uncertainty (%)	11.5 %	38.7 %	9.4 %

For NIST RM 8013:	**Reported diameter (ROI)** (*PNC_{direct}/PNC_{mean}*) **106.0 %**	**HR-SEM diameter** (*PNC_{direct}/PNC_{mean}*) **102.7 %**	**spICP-MS diameter** (*PNC_{direct}/PNC_{mean}*) **97.7 %**
Source of uncertainty	**Relative contribution (%)**	**Relative contribution (%)**	**Relative contribution (%)**
Particle size consensus value for standard ($d_{NP\ RM}$)	16.8	0.6	0.1
Dilution Factor of stock suspension for the sample (*Dil.F*)	0.2	< 0.0	< 0.0
Measurement repeatability (*Rep*)	1.5	0.1	< 0.0
Number of observed events for the sample (N_{NP})	6.3	0.2	0.1
Au mass fraction of the standard ($C_{S\ RM}$)	0.1	< 0.0	< 0.0
Sample uptake rate for the standard ($q_{liq\ RM}$)	0.1	< 0.0	< 0.0
Time of acquisition for the standard ($t_{aq\ RM}$)	< 0.0	< 0.0	< 0.0
Number of observed events for the standard ($N_{NP\ RM}$)	12.3	0.4	0.1
Sample uptake rate for the sample (q_{liq})	0.1	< 0.0	< 0.0
Time of acquisition for the sample (t_{aq})	< 0.0	< 0.0	< 0.0
Dilution Factor of stock suspension for the standard ($Dil.F_{RM}$)	0.4	< 0.0	< 0.0
Particle size for the sample (d_{NP})	51.2	97.4	95.4
Au mass fraction of the sample (C_S)	10.7	0.4	0.1
Density of the particles (ρ)	0.1	< 0.0	< 0.0
Residual	0.2	0.9	4.2
Combined standard uncertainty (%)	2.0 %	10.5 %	22.2 %
Expanded k=2 uncertainty (%)	4.0 %	21.0 %	44.4 %

Table S-9. Uncertainty budget for the calculation of $PNC_{distribution}$ of NIST RM 8012 and RM 8013. Full particle size distribution reported by TEM (NIST ROIs)[2,3] (first column), HR-SEM[1] (second column), and spICP-MS[1] (third column) for NIST RMs were combined with Au mass fraction[2,3] to derive $PNC_{distribution}$.

For NIST RM 8012:	**TEM (ROI) ($PNC_{distribution}$ 2.63 x 10^{14} L^{-1})**	**HR-SEM ($PNC_{distribution}$ 2.47 x 10^{14} L^{-1})**	**spICP-MS ($PNC_{distribution}$ 2.76 x 10^{14} L^{-1})**
Source of uncertainty	**Relative contribution (%)**	**Relative contribution (%)**	**Relative contribution (%)**
Au mass fraction of the material (C_S)	0.3	< 0.0	0.6
Particle size for the material ($d_{NP\ RM}$)	95.3	96.9	94.9
Density of the particles (ρ)	< 0.0	< 0.0	< 0.0
Spread of particle size distribution	4.1	< 0.0	4.2
Residual	0.3	3.0	0.3
Combined standard uncertainty (L^{-1})	1.6 x 10^{13} L^{-1}	4.7 x 10^{13} L^{-1}	1.4 x 10^{13} L^{-1}
Expanded k=2 uncertainty (L^{-1})	3.1 x 10^{13} L^{-1}	9.4 x 10^{13} L^{-1}	2.9 x 10^{13} L^{-1}

For NIST RM 8013:	**TEM (ROI) ($PNC_{distribution}$ 3.10 x 10^{13} L^{-1})**	**HR-SEM ($PNC_{distribution}$ 3.14 x 10^{13} L^{-1})**	**spICP-MS ($PNC_{distribution}$ 3.37 x 10^{13} L^{-1})**
Source of uncertainty	**Relative contribution (%)**	**Relative contribution (%)**	**Relative contribution (%)**
Au mass fraction of the material (C_S)	11.7	0.4	0.1
Particle size for the material ($d_{NP\ RM}$)	56.0	98.6	95.7
Density of the particles (ρ)	0.1	< 0.0	< 0.0
Spread of particle size distribution	32.3	0.1	0.1
Residual	< 0.0	0.9	4.2
Combined standard uncertainty (L^{-1})	0.07 x 10^{13} L^{-1}	0.31 x 10^{13} L^{-1}	0.7 x 10^{13} L^{-1}
Expanded k=2 uncertainty (L^{-1})	0.13 x 10^{13} L^{-1}	0.62 x 10^{13} L^{-1}	1.5 x 10^{13} L^{-1}

Table S-10. Uncertainty budget for the ratio between PNC_{direct} obtained across 15 independent spICP-MS experiments, expressed in percentage, and $PNC_{distribution}$ for RM 8012 and RM 8013. $PNC_{distribution}$ values reported for purposes of comparison to PNC_{direct} were derived based on the combination of Au mass fraction and the full size distribution of particle diameters reported by TEM (NIST ROIs)[2,3] (first column), HR-SEM[1] (second column), and spICP-MS[1] (third column).

For NIST RM 8012:	**TEM (ROI)** ($PNC_{direct}/PNC_{distribution}$) **90.4 %**	**HR-SEM** ($PNC_{direct}/PNC_{distribution}$) **96.5 %**	**spICP-MS** ($PNC_{direct}/PNC_{distribution}$) **86.1 %**
Source of uncertainty	**Relative contribution (%)**	**Relative contribution (%)**	**Relative contribution (%)**
Particle size consensus value for standard ($d_{NP\ RM}$)	0.3	< 0.0	0.3
Dilution Factor of stock suspension for the sample ($Dil.F$)	0.1	< 0.0	0.1
Measurement repeatability (Rep)	0.4	< 0.0	0.5
Number of observed events for the sample (N_{NP})	3.3	0.3	4.2
Au mass fraction of the standard ($C_{S\ RM}$)	0.1	< 0.0	0.1
Sample uptake rate for the standard ($q_{liq\ RM}$)	< 0.0	< 0.0	< 0.0
Time of acquisition for the standard ($t_{aq\ RM}$)	< 0.0	< 0.0	< 0.0
Number of observed events for the standard ($N_{NP\ RM}$)	1.8	0.2	2.2
Sample uptake rate for the sample (q_{liq})	< 0.0	< 0.0	< 0.0
Time of acquisition for the sample (t_{aq})	< 0.0	< 0.0	< 0.0
Dilution Factor of stock suspension for the standard ($Dil.F_{RM}$)	0.1	0.1	0.1
Particle size for the sample (d_{NP})	89.5	96.3	87.7
Au mass fraction of the sample (C_S)	0.3	< 0.0	0.5
Density of the particles (ρ)	< 0.0	< 0.0	< 0.0
Spread of the particle size distribution	3.8	< 0.0	3.9
Residual	0.3	3.0	0.3
Combined standard uncertainty (%)	5.5 %	18.5 %	4.7 %
Expanded k=2 uncertainty (%)	N/A	37.0 %	9.4 %

For NIST RM 8013:	**TEM (ROI)** (***PNC_{direct}/$PNC_{distribution}$***) **102.1 %**	**HR-SEM** (***PNC_{direct}/$PNC_{distribution}$***) **100.8 %**	**spICP-MS** (***PNC_{direct}/$PNC_{distribution}$***) **93.9 %**
Source of uncertainty	**Relative contribution (%)**	**Relative contribution (%)**	**Relative contribution (%)**
Particle size consensus value for standard ($d_{\mathrm{NP\ RM}}$)	9.7	0.6	0.1
Dilution Factor of stock suspension for the sample (*Dil.F*)	0.1	< 0.0	< 0.0
Measurement repeatability (*Rep*)	0.8	0.1	< 0.0
Number of observed events for the sample (N_{NP})	3.6	0.2	0.1
Au mass fraction of the standard ($C_{S\ RM}$)	< 0.0	< 0.0	< 0.0
Sample uptake rate for the standard ($q_{liq\ RM}$)	0.1	< 0.0	< 0.0
Time of acquisition for the standard ($\mathrm{t}_{aq\ RM}$)	< 0.0	< 0.0	< 0.0
Number of observed events for the standard ($N_{NP\ RM}$)	7.0	0.4	0.1
Sample uptake rate for the sample (q_{liq})	0.1	< 0.0	< 0.0
Time of acquisition for the sample (t_{aq})	< 0.0	< 0.0	< 0.0
Dilution Factor of stock suspension for the standard ($Dil.F_{RM}$)	0.2	< 0.0	< 0.0
Particle size for the sample (d_{NP})	43.8	97.3	95.4
Au mass fraction of the sample (C_S)	9.1	0.4	0.1
Density of the particles (ρ)	< 0.0	< 0.0	< 0.0
Spread of the particle size distribution	25.2	0.1	< 0.0
Residual	0.1	0.9	4.2
Combined standard uncertainty (%)	2.5%	10.1 %	20.8 %
Expanded k=2 uncertainty (%)	N/A	20.1 %	41.5 %

Table S-11. Huber estimates of particle size location (or central tendency) by spICP-MS simultaneously obtained with the PNC measurements and comparison with reference spICP-MS results previously published[1] for NIST RM 8012 and 8013, for different commercial AuNPs.

	spICP-MS	Difference vs Reference[1]
RM 8012 (nm)	26.9 ± 0.07 (0.1)[a]	-1.3 %
NPs analyzed	51159	
MAD (nm)	2.0	
RM 8013 (nm)	55.2 ± 0.1 (0.3)[a]	2.0 %
NPs analyzed	53247	
MAD (nm)	3.1	
30 nm PVP (nm)	30.9 ± 0.2 (0.6)[a]	3.1 %
NPs analyzed	1791	
MAD (nm)	2.2	
30 nm bPEI (nm)	31.5 ± 0.2 (1.3)[a]	1.6 %
NPs analyzed	1914	
MAD (nm)	3.4	
30 nm PEG (nm)	30.7 ± 0.1 (0.9)[a]	0.2 %
NPs analyzed	2704	
MAD (nm)	2.9	
60 nm PVP (nm)	60.8 ± 0.4 (1.1)[a]	3.7 %
NPs analyzed	1352	
MAD (nm)	8.2	
60 nm bPEI first lot (nm)	60.7 ± 0.3 (0.9)[a]	0.8 %
NPs analyzed	4014	
MAD (nm)	9.4	
60 nm bPEI second lot (nm)	60.3 ± 0.3 (1.0)[a]	2.6 %
NPs analyzed	4565	
MAD (nm)	8.6	
60 nm PEG firs lot (nm)	55.9 ± 0.3 (1.0)[a]	-1.4 %
NPs analyzed	3421	
MAD (nm)	8.6	

60 nm PEG second lot (nm)	60.5 ± 0.3 (3.)[a]	3.8 %
NPs analyzed	3346	
MAD (nm)	8.1	
100 nm Citrate (nm)	93.3 ± 0.6 (2.3)[a]	0.1 %
NPs analyzed	2820	
MAD (nm)	14.7	
100 nm PVP (nm)	96.7 ± 0.6 (3.3)[a]	1.2 %
NPs analyzed	1891	
MAD (nm)	10.8	
100 nm bPEI (nm)	94.9 ± 0.5 (2.0)[a]	0.5 %
NPs analyzed	2924	
MAD (nm)	11.2	
100 nm PEG (nm)	99.9 ± 0.7 (3.0)[a]	1.2 %
NPs analyzed	2382	
MAD (nm)	14.9	

Values indicate the Huber estimates of particle size location, and the standard uncertainty associated with the Huber estimate.

[a]All the components affecting spICP-MS and HR-SEM size determinations were included in the parenthetical uncertainty computation.

Table S-12. PNCs derived for NIST AuNP RMs using Au mass fraction reported in the NIST ROIs[2,3] and: Huber estimates of particle size location (or central tendency) (first column), and the full particle size distribution (second column) simultaneously measured by spICP-MS across 15 independent experiments.

	Central Tendency (PNC_{mean})[a]	Full PSD ($PNC_{distribution}$)
RM 8012		
spICP-MS[b]	$2.46 \times 10^{14} \pm 0.04 \times 10^{14}$ L^{-1}	$2.74 \times 10^{14} \pm 0.12 \times 10^{14}$ L^{-1}
RM 8013		
spICP-MS[b]	$3.04 \times 10^{13} \pm 0.06 \times 10^{13}$ L^{-1}	$3.35 \times 10^{13} \pm 0.07 \times 10^{13}$ L^{-1}

[a] Assumes all analyte is present as spherical NPs of the central tendency diameter.

[b] Expanded uncertainties associated with the spICP-MS size determinations included a best estimate of known or suspected sources of bias. Listed uncertainties are based on a confidence interval, with the coverage factor, k = 2 corresponding to approximately 95 % confidence.

Table S-13. Uncertainty budget for the calculation of PNC_{mean} of NIST RM 8012 and RM 8013 derived based on the combination of Au mass fraction[2,3] and the Huber estimates of particle size (or central tendency) results simultaneously obtained by spICP-MS in this study.

For NIST RM 8012:	**spICP-MS simultaneous (PNC_{mean} 2.46 x 10^{14} L^{-1})**
Source of uncertainty	**Relative contribution (%)**
Au mass fraction of the material (C_S)	17.3
Particle size for the material ($d_{NP\ RM}$)	82.3
Density of the particles (ρ)	0.4
Residual	< 0.0
Combined standard uncertainty (L^{-1})	0.2 x 10^{13} L^{-1}
Expanded k=2 uncertainty (L^{-1})	0.4 x 10^{13} L^{-1}

For NIST RM 8013:	**spICP-MS simultaneous (PNC_{mean} 3.04 x 10^{13} L^{-1})**
Source of uncertainty	**Relative contribution (%)**
Au mass fraction of the material (C_S)	45.1
Particle size for the material ($d_{NP\ RM}$)	54.6
Density of the particles (ρ)	0.3
Residual	< 0.0
Combined standard uncertainty (L^{-1})	0.3 x 10^{12} L^{-1}
Expanded k=2 uncertainty (L^{-1})	0.6 x 10^{12} L^{-1}

Table S-14. Uncertainty budget for the ratio between PNC_{direct} obtained across 15 independent spICP-MS experiments, expressed in percentage, and PNC_{mean} for RM 8012 and RM 8013. PNC_{mean} values reported for purposes of comparison to PNC_{direct} were derived based on the combination of Au mass fraction and the Huber estimates of particle size (or central tendency) results simultaneously obtained by spICP-MS in this study.

	RM 8012 (PNC_{direct}/PNC_{mean}) 96.9 %	**RM 8013 (PNC_{direct}/PNC_{mean}) 103.9 %**
Source of uncertainty	**Relative contribution (%)**	**Relative contribution (%)**
Particle size consensus value for standard ($d_{NP\ RM}$)	3.3	27.3
Dilution Factor of stock suspension for the sample (*Dil.F*)	1.4	0.4
Measurement repeatability (*Rep*)	5.1	2.4
Number of observed events for the sample (N_{NP})	42.4	10.3
Au mass fraction of the standard ($C_{S\ RM}$)	0.7	0.1
Sample uptake rate for the standard ($q_{liq\ RM}$)	0.4	0.2
Time of acquisition for the standard ($t_{aq\ RM}$)	< 0.0	< 0.0
Number of observed events for the standard ($N_{NP\ RM}$)	22.4	19.9
Sample uptake rate for the sample (q_{liq})	0.4	0.2
Time of acquisition for the sample (t_{aq})	< 0.0	< 0.0
Dilution Factor of stock suspension for the standard ($Dil.F_{RM}$)	0.8	0.6
Particle size for the sample (d_{NP})	18.8	20.9
Au mass fraction of the sample (C_S)	4.0	17.2
Density of the particles (ρ)	0.1	0.1
Residual	0.2	0.3
Combined standard uncertainty (%)	1.7 %	1.5 %
Expanded k=2 uncertainty (%)	3.3 %	3.1 %

Table S-15. Uncertainty budget for the calculation of $PNC_{distribution}$ of NIST RM 8012 and RM 8013 derived based on the combination of Au mass fraction[2,3] and a representative full particle size distribution simultaneously obtained by spICP-MS in this study.

	RM 8012 ($PNC_{distribution}$ 2.74 x 10^{14} L^{-1})	**RM 8013 ($PNC_{distribution}$ 3.35 x 10^{13} L^{-1})**
Source of uncertainty	**Relative contribution (%)**	**Relative contribution (%)**
Au mass fraction of the material (C_S)	14.0	44.8
Particle size for the material ($d_{NP\ RM}$)	66.5	54.3
Density of the particles (ρ)	0.3	0.3
Spread of particle size distribution	19.2	0.5
Residual	< 0.0	< 0.0
Combined standard uncertainty (L^{-1}) Expanded k=2 uncertainty (L^{-1})	0.6 x 10^{13} L^{-1} 1.2 x 10^{13} L^{-1}	0.2 x 10^{12} L^{-1} 0.7 x 10^{12} L^{-1}

Table S-16. Uncertainty budget for the ratio between *PNC_{direct}*, obtained across 15 independent spICP-MS experiments, expressed in percentage, and *$PNC_{distribution}$* for RM 8012 and RM 8013. *$PNC_{distribution}$* values reported for purposes of comparison to *PNC_{direct}* were derived based on the combination of Au mass fraction[2,3] and a representative full particle size distribution simultaneously obtained by spICP-MS in this study.

	RM 8012 ($PNC_{direct}/PNC_{distribution}$) **87.0 %**	**RM 8013** ($PNC_{direct}/PNC_{distribution}$) **94.4 %**
Source of uncertainty	**Relative contribution (%)**	**Relative contribution (%)**
Particle size consensus value for standard ($d_{\mathrm{NP\,RM}}$)	1.3	23.2
Dilution Factor of stock suspension for the sample (*Dil.F*)	0.6	0.3
Measurement repeatability (*Rep*)	2.1	2.0
Number of observed events for the sample (N_{NP})	17.4	8.7
Au mass fraction of the standard ($C_{S\,RM}$)	0.3	0.1
Sample uptake rate for the standard ($q_{liq\,RM}$)	0.2	0.2
Time of acquisition for the standard ($t_{aq\,RM}$)	< 0.0	< 0.0
Number of observed events for the standard ($N_{NP\,RM}$)	9.2	16.9
Sample uptake rate for the sample (q_{liq})	0.2	0.2
Time of acquisition for the sample (t_{aq})	< 0.0	< 0.0
Dilution Factor of stock suspension for the standard ($Dil.F_{RM}$)	0.3	0.5
Particle size for the sample (d_{NP})	45.5	25.8
Au mass fraction of the sample (C_S)	9.6	21.3
Density of the particles (ρ)	0.2	0.2
Spread of the particle size distribution	13.1	0.2
Residual	0.1	0.3
Combined standard uncertainty (%)	2.3 %	1.5 %
Expanded k=2 uncertainty (%)	4.6 %	3.0 %

Table S-17. Average uncertainty budget for spICP-MS determination of PNC_{direct} of 30 nm, 60 nm, and 100 nm commercial AuNPs, respectively, using NIST RM 8013 as the calibration standard.

Source of uncertainty	30 nm AuNPs (Av PNC_{direct} 2.13 x 10^{14} L^{-1}) Relative contribution (%)	60 nm AuNPs (Av PNC_{direct} 2.72 x 10^{13} L^{-1}) Relative contribution (%)	100 nm AuNPs (Av PNC_{direct} 5.42 x 10^{12} L^{-1}) Relative contribution (%)
Particle size consensus value for RM 8013 ($d_{NP\ RM}$)	5.9	5.0	5.1
Dilution Factor of stock suspension for the sample (*Dil.F*)	10.2	2.1	9.8
Measurement repeatability (*Rep*)	9.2	7.9	8.0
Number of observed events for the sample (N_{NP})	36.8	25.5	38.8
Au mass fraction of RM 8013 (C_S)	1.2	1.0	1.0
Sample uptake rate for RM 8013 ($q_{liq\ RM}$)	0.9	0.7	0.7
Time of acquisition for RM 8013 ($t_{aq\ RM}$)	< 0.0	< 0.0	< 0.0
Number of observed events for RM8013 ($N_{NP\ RM}$)	29.8	52.0	26.1
Sample uptake rate for the sample (q_{liq})	0.9	0.7	0.7
Time of acquisition for the sample (t_{aq})	< 0.0	< 0.0	< 0.0
Dilution Factor of stock suspension for RM 8013 ($Dil.F_{RM}$)	5.0	4.6	10.1
Density of the particles (ρ)	< 0.0	< 0.0	< 0.0
Residual	0.2	0.4	0.2
Combined standard uncertainty (L^{-1})	1.0 x 10^{13} L^{-1}	0.8 x 10^{12} L^{-1}	2.1 x 10^{11} L^{-1}
Expanded k=2 uncertainty (L^{-1})	2.9 x 10^{13} L^{-1}	3.5 x 10^{12} L^{-1}	6.6 x 10^{11} L^{-1}

Table S-18. Total Au mass fraction provided by the supplier,[16] and in-house measurements for different commercial AuNPs analyzed in this study.

	Supplier Au mass fraction	In-house Au mass fraction
30 nm PVP	50	61.65 ± 3.67
30 nm bPEI	52	62.07 ± 2.23
30 nm PEG	51	57.45 ± 1.45
60 nm PVP	54	59.66 ± 3.90
60 nm bPEI first lot	52	59.77 ± 6.19
60 nm bPEI second lot	53	63.68 ± 1.04
60 nm PEG first lot	53	57.26 ± 0.49
60 nm PEG second lot	50	56.97 ± 0.76
100 nm Citrate	52	51.47 ± 2.66
100 nm PVP	52	44.30 ± 1.56
100 nm bPEI	52	41.92 ± 3.49
100 nm PEG	54	59.18 ± 0.82

Values indicate the mean and 1 SD, n=3

Table S-19. PNCs derived for different commercial AuNPs based on the combination of Au mass fraction with: (first column) the Huber estimates of particle size location (or central tendency), and the full particle size distribution reported by TEM (second column) (supplier),[16] HR-SEM,[1] and spICP-MS.[1] Note that PNCs derived from the combination of Au mass fraction with TEM size provided by the supplier were reported in the first row for each material, while in-house Au mass fraction determinations were used for the remainder rows.

	Central Tendency (PNC_{mean})[a]	Full PSD ($PNC_{distribution}$)
30 nm PVP		
TEM + Au mass fraction (supplier)	$1.87 \times 10^{14} \pm 0.24 \times 10^{14} L^{-1}$	$2.00 \times 10^{14} \pm 0.30 \times 10^{14} L^{-1}$ [c]
TEM (supplier) + in-house Au mass fraction	$2.31 \times 10^{14} \pm 0.33 \times 10^{14} L^{-1}$	$2.47 \times 10^{14} \pm 0.40 \times 10^{14} L^{-1}$ [c]
HR-SEM[b]	$2.38 \times 10^{14} \pm 0.84 \times 10^{14} L^{-1}$	$2.69 \times 10^{14} \pm 0.95 \times 10^{14} L^{-1}$
spICP-MS[b]	$2.26 \times 10^{14} \pm 0.30 \times 10^{14} L^{-1}$	$2.75 \times 10^{14} \pm 0.41 \times 10^{14} L^{-1}$
30 nm bPEI		
TEM + Au mass fraction (supplier)	$1.76 \times 10^{14} \pm 0.27 \times 10^{14} L^{-1}$	$1.84 \times 10^{14} \pm 0.30 \times 10^{14} L^{-1}$ [c]
TEM (supplier) + in-house Au mass fraction	$2.10 \times 10^{14} \pm 0.29 \times 10^{14} L^{-1}$	$2.19 \times 10^{14} \pm 0.33 \times 10^{14} L^{-1}$ [c]
HR-SEM[b]	$1.97 \times 10^{14} \pm 0.65 \times 10^{14} L^{-1}$	$2.48 \times 10^{14} \pm 0.82 \times 10^{14} L^{-1}$
spICP-MS[b]	$2.06 \times 10^{14} \pm 0.19 \times 10^{14} L^{-1}$	$2.54 \times 10^{14} \pm 0.29 \times 10^{14} L^{-1}$
30 nm PEG		
TEM + Au mass fraction (supplier)	$1.46 \times 10^{14} \pm 0.21 \times 10^{14} L^{-1}$	$1.56 \times 10^{14} \pm 0.24 \times 10^{14} L^{-1}$ [c]
TEM (supplier) + in-house Au mass fraction	$1.64 \times 10^{14} \pm 0.20 \times 10^{14} L^{-1}$	$1.75 \times 10^{14} \pm 0.24 \times 10^{14} L^{-1}$ [c]
HR-SEM[b]	$2.13 \times 10^{14} \pm 0.71 \times 10^{14} L^{-1}$	$2.46 \times 10^{14} \pm 0.82 \times 10^{14} L^{-1}$
spICP-MS[b]	$1.98 \times 10^{14} \pm 0.17 \times 10^{14} L^{-1}$	$2.49 \times 10^{14} \pm 0.25 \times 10^{14} L^{-1}$
60 nm PVP		
TEM + Au mass fraction (supplier)	$2.99 \times 10^{13} \pm 0.59 \times 10^{13} L^{-1}$	$3.54 \times 10^{13} \pm 0.81 \times 10^{13} L^{-1}$ [c]
TEM (supplier) + in-house Au mass fraction	$3.31 \times 10^{13} \pm 0.70 \times 10^{13} L^{-1}$	$3.91 \times 10^{13} \pm 0.94 \times 10^{13} L^{-1}$ [c]
HR-SEM[b]	$2.79 \times 10^{13} \pm 0.63 \times 10^{13} L^{-1}$	$3.30 \times 10^{13} \pm 0.75 \times 10^{13} L^{-1}$
spICP-MS[b]	$2.93 \times 10^{13} \pm 0.40 \times 10^{13} L^{-1}$	$3.52 \times 10^{13} \pm 0.49 \times 10^{13} L^{-1}$
60 nm bPEI first lot		

TEM + Au mass fraction (supplier)	1.93 x 10^{13} ± 0.33 x 10^{13} L^{-1}	2.19 x 10^{13} ± 0.42 x 10^{13} L^{-1} [c]
TEM (supplier) + in-house Au mass fraction	2.21 x 10^{13} ± 0.55 x 10^{13} L^{-1}	2.52 x 10^{13} ± 0.67 x 10^{13} L^{-1} [c]
HR-SEM[b]	2.69 x 10^{13} ± 0.74 x 10^{13} L^{-1}	2.97 x 10^{13} ± 0.81 x 10^{13} L^{-1}
spICP-MS[b]	2.71 x 10^{13} ± 0.57 x 10^{13} L^{-1}	3.04 x 10^{13} ± 0.64 x 10^{13} L^{-1}
60 nm bPEI second lot		
TEM + Au mass fraction (supplier)	2.24 x 10^{13} ± 0.38 x 10^{13} L^{-1}	2.47 x 10^{13} ± 0.45 x 10^{13} L^{-1} [c]
TEM (supplier) + in-house Au mass fraction	2.70 x 10^{13} ± 0.37 x 10^{13} L^{-1}	2.96 x 10^{13} ± 0.46 x 10^{13} L^{-1} [c]
HR-SEM[b]	3.08 x 10^{13} ± 0.57 x 10^{13} L^{-1}	3.38x 10^{13} ± 0.63 x 10^{13} L^{-1}
spICP-MS[b]	3.10 x 10^{13} ± 0.21 x 10^{13} L^{-1}	3.59 x 10^{13} ± 0.25 x 10^{13} L^{-1}
60 nm PEG first lot		
TEM + Au mass fraction (supplier)	1.87 x 10^{13} ± 0.33 x 10^{13} L^{-1}	2.09 x 10^{13} ± 0.41 x 10^{13} L^{-1} [c]
TEM (supplier) + in-house Au mass fraction	2.02 x 10^{13} ± 0.30 x 10^{13} L^{-1}	2.26 x 10^{13} ± 0.39 x 10^{13} L^{-1} [c]
HR-SEM[b]	2.94 x 10^{13} ± 0.55 x 10^{13} L^{-1}	3.83 x 10^{13} ± 0.82 x 10^{13} L^{-1}
spICP-MS[b]	3.11 x 10^{13} ± 0.14 x 10^{13} L^{-1}	3.66 x 10^{13} ± 0.19 x 10^{13} L^{-1}
60 nm PEG second lot		
TEM + Au mass fraction (supplier)	1.84 x 10^{13} ± 0.31 x 10^{13} L^{-1}	2.04 x 10^{13} ± 0.38 x 10^{13} L^{-1} [c]
TEM (supplier) + in-house Au mass fraction	2.09 x 10^{13} ± 0.29 x 10^{13} L^{-1}	2.33 x 10^{13} ± 0.38 x 10^{13} L^{-1} [c]
HR-SEM[b]	2.65 x 10^{13} ± 0.49 x 10^{13} L^{-1}	3.07 x 10^{13} ± 0.57 x 10^{13} L^{-1}
spICP-MS[b]	2.85 x 10^{13} ± 0.43 x 10^{13} L^{-1}	3.26 x 10^{13} ± 0.50 x 10^{13} L^{-1}
100 nm Citrate		
TEM + Au mass fraction (supplier)	4.44 x 10^{12} ± 0.79 x 10^{12} L^{-1}	5.09 x 10^{12} ± 1.02 x 10^{12} L^{-1} [c]
TEM (supplier) + in-house Au mass fraction	4.40 x 10^{12} ± 0.79 x 10^{12} L^{-1}	5.03 x 10^{12} ± 1.02 x 10^{12} L^{-1} [c]
HR-SEM[b]	5.28 x 10^{12} ± 0.90 x 10^{12} L^{-1}	6.24 x 10^{12} ± 1.07 x 10^{12} L^{-1}
spICP-MS[b]	6.29 x 10^{12} ± 0.76 x 10^{12} L^{-1}	7.45 x 10^{12} ± 0.92 x 10^{12} L^{-1}
100 nm PVP		
TEM + Au mass fraction (supplier)	5.11 x 10^{12} ± 0.66 x 10^{12} L^{-1}	5.33 x 10^{12} ± 0.74 x 10^{12} L^{-1} [c]
TEM (supplier) + in-house Au mass fraction	4.36 x 10^{12} ± 0.47 x 10^{12} L^{-1}	4.54 x 10^{12} ± 0.54 x 10^{12} L^{-1} [c]
HR-SEM[b]	5.03 x 10^{12} ± 0.77 x 10^{12} L^{-1}	5.51 x 10^{12} ± 0.84 x 10^{12} L^{-1}
spICP-MS[b]	5.03 x 10^{12} ± 0.65 x 10^{12} L^{-1}	6.34 x 10^{12} ± 0.86 x 10^{12} L^{-1}
100 nm bPEI		

TEM + Au mass fraction (supplier)	$5.28 \times 10^{12} \pm 0.87 \times 10^{12} L^{-1}$	$5.90 \times 10^{12} \pm 1.08 \times 10^{12} L^{-1}$ [c]
TEM (supplier) + in-house Au mass fraction	$4.26 \times 10^{12} \pm 0.90 \times 10^{12} L^{-1}$	$4.76 \times 10^{12} \pm 1.07 \times 10^{12} L^{-1}$ [c]
HR-SEM[b]	$4.71 \times 10^{12} \pm 0.98 \times 10^{12} L^{-1}$	$5.47 \times 10^{12} \pm 1.14 \times 10^{12} L^{-1}$
spICP-MS[b]	$4.94 \times 10^{12} \pm 0.90 \times 10^{12} L^{-1}$	$5.65 \times 10^{12} \pm 1.04 \times 10^{12} L^{-1}$
100 nm PEG		
TEM + Au mass fraction (supplier)	$4.55 \times 10^{12} \pm 0.85 \times 10^{12} L^{-1}$	$5.51 \times 10^{12} \pm 1.27 \times 10^{12} L^{-1}$ [c]
TEM (supplier) + in-house Au mass fraction	$4.99 \times 10^{12} \pm 0.80 \times 10^{12} L^{-1}$	$6.04 \times 10^{12} \pm 1.26 \times 10^{12} L^{-1}$ [c]
HR-SEM[b]	$6.96 \times 10^{12} \pm 0.98 \times 10^{12} L^{-1}$	$7.87 \times 10^{12} \pm 1.12 \times 10^{12} L^{-1}$
spICP-MS[b]	$6.07 \times 10^{12} \pm 0.71 \times 10^{12} L^{-1}$	$7.22 \times 10^{12} \pm 0.86 \times 10^{12} L^{-1}$

[a] Assumes all analyte is present as spherical NPs of the central tendency diameter.

[b] Expanded uncertainties associated with the spICP-MS and HR-SEM size determinations included a best estimate of known or suspected sources of bias.[1]

[c] PNC derived from the full particle size distribution obtained by TEM (supplier).[16]

Listed uncertainties are based on a confidence interval, with the coverage factor, k = 2 corresponding to approximately 95 % confidence.

Table S-20. Average uncertainty budget for the calculation of *PNC_{mean}* of 30 nm, 60 nm, and 100 nm commercial AuNPs, respectively. The Huber estimates of particle size (or central tendency) reported by TEM[16] (supplier) (first column), HR-SEM[1] (second column), and spICP-MS[1] (third column) were combined with in-house Au mass fraction determinations to derive *PNC_{mean}*.

For 30 nm AuNPs:	**TEM (Supplier) (*PNC_{mean}* 2.02 x 10^{14} L^{-1})**	**HR-SEM (*PNC_{mean}* 2.16 x 10^{14} L^{-1})**	**spICP-MS (*PNC_{mean}* 2.10 x 10^{14} L^{-1})**
Source of uncertainty	**Relative contribution (%)**	**Relative contribution (%)**	**Relative contribution (%)**
Au mass fraction of the material (C_S)	37.7	6.2	58.4
Particle size for the material (d_{NP})	62.0	91.5	41.5
Density of the particles (ρ)	< 0.0	< 0.0	< 0.0
Residual	0.3	2.4	0.1
Combined standard uncertainty (L^{-1})	1.4 x 10^{13} L^{-1}	3.6 x 10^{13} L^{-1}	1.1 x 10^{13} L^{-1}
Expanded k=2 uncertainty (L^{-1})	2.7 x 10^{13} L^{-1}	7.3 x 10^{13} L^{-1}	2.2 x 10^{13} L^{-1}

For 60 nm AuNPs:	**TEM (Supplier) (*PNC_{mean}* 2.47 x 10^{13}·L^{-1})**	**HR-SEM (*PNC_{mean}* 2.83 x 10^{13} L^{-1})**	**spICP-MS (*PNC_{mean}* 2.94 x 10^{13} L^{-1})**
Source of uncertainty	**Relative contribution (%)**	**Relative contribution (%)**	**Relative contribution (%)**
Au mass fraction of the material (C_S)	23.0	18.8	44.3
Particle size for the material (d_{NP})	76.4	80.4	55.5
Density of the particles (ρ)	< 0.0	< 0.0	< 0.0
Residual	0.5	0.8	0.2
Combined standard uncertainty (L^{-1})	2.3 x 10^{12} L^{-1}	3.0 x 10^{12} L^{-1}	1.8 x 10^{12} L^{-1}
Expanded k=2 uncertainty (L^{-1})	4.4 x 10^{12} L^{-1}	6.0 x 10^{12} L^{-1}	3.5 x 10^{12} L^{-1}

For 100 nm AuNPs:	TEM (Supplier) (PNC_{mean} 4.50 x 10^{12} L^{-1})	HR-SEM (PNC_{mean} 5.50 x 10^{12} L^{-1})	spICP-MS (PNC_{mean} 5.58 x 10^{12} L^{-1})
Source of uncertainty	**Relative contribution (%)**	**Relative contribution (%)**	**Relative contribution (%)**
Au mass fraction of the material (C_S)	34.3	29.9	47.0
Particle size for the material (d_{NP})	65.3	69.7	52.8
Density of the particles (ρ)	< 0.0	< 0.0	< 0.0
Residual	0.4	0.4	0.2
Combined standard uncertainty (L^{-1})	3.7 x 10^{11} L^{-1}	4.6 x 10^{11} L^{-1}	3.8 x 10^{11} L^{-1}
Expanded k=2 uncertainty (L^{-1})	7.4 x 10^{11} L^{-1}	9.1 x 10^{11} L^{-1}	7.5 x 10^{11} L^{-1}

Table S-21. Average uncertainty budget for the ratio between PNC_{direct} and PNC_{mean}, expressed in percentage, for 30 nm, 60 nm, and 100 nm commercial AuNPs, respectively. PNC_{mean} values were derived based on the combination of in-house Au mass fraction and the Huber estimates of particle size (or central tendency) reported by TEM (supplier)[16] (first column), HR-SEM[1] (second column), and spICP-MS[1] (third column).

For 30 nm AuNPs:	**TEM (Supplier)** (PNC_{direct}/PNC_{mean}) **107.7 %**	**HR-SEM** (PNC_{direct}/PNC_{mean}) **98.8 %**	**spICP-MS** (PNC_{direct}/PNC_{mean}) **101.4 %**
Source of uncertainty	**Relative contribution (%)**	**Relative contribution (%)**	**Relative contribution (%)**
Particle size consensus value for standard ($d_{NP\ RM}$)	2.6	0.7	3.2
Dilution Factor of stock suspension for the sample (*Dil.F*)	5.9	2.0	7.4
Measurement repeatability (*Rep*)	4.1	1.2	5.0
Number of observed events for the sample (N_{NP})	21.3	6.1	27.0
Au mass fraction of the standard ($C_{S\ RM}$)	0.5	0.2	0.6
Sample uptake rate for the standard ($q_{liq\ RM}$)	0.4	0.1	0.5
Time of acquisition for the standard ($t_{aq\ RM}$)	< 0.0	< 0.0	< 0.0
Number of observed events for the standard ($N_{NP\ RM}$)	11.7	3.3	13.9
Sample uptake rate for the sample (q_{liq})	0.4	0.1	0.5
Time of acquisition for the sample (t_{aq})	< 0.0	< 0.0	< 0.0
Dilution Factor of stock suspension for the standard ($Dil.F_{RM}$)	2.9	1.0	3.6
Particle size for the sample (d_{NP})	27.9	77.8	12.9
Au mass fraction of the sample (C_S)	22.1	5.4	25.3
Density of the particles (ρ)	< 0.0	< 0.0	< 0.0
Residual	0.2	2.1	0.2
Combined standard uncertainty (%)	9.1 %	17.4 %	7.6 %
Expanded k=2 uncertainty (%)	N/A	34.8 %	15.2 %

For 60 nm AuNPs:	TEM (Supplier) (PNC_{direct}/PNC_{mean}) 114.3 %	HR-SEM (PNC_{direct}/PNC_{mean}) 96.1 %	spICP-MS (PNC_{direct}/PNC_{mean}) 92.4 %
Source of uncertainty	**Relative contribution (%)**	**Relative contribution (%)**	**Relative contribution (%)**
Particle size consensus value for standard ($d_{\mathrm{NP\ RM}}$)	1.5	1.2	2.4
Dilution Factor of stock suspension for the sample ($Dil.F$)	0.2	0.5	0.9
Measurement repeatability (Rep)	2.4	1.8	3.8
Number of observed events for the sample (N_{NP})	10.2	7.5	14.4
Au mass fraction of the standard ($C_{S\ RM}$)	0.3	0.2	0.5
Sample uptake rate for the standard ($q_{liq\ RM}$)	0.2	0.2	0.3
Time of acquisition for the standard ($t_{aq\ RM}$)	< 0.0	< 0.0	< 0.0
Number of observed events for the standard ($N_{NP\ RM}$)	20.2	15.5	30.3
Sample uptake rate for the sample (q_{liq})	0.2	0.2	0.3
Time of acquisition for the sample (t_{aq})	< 0.0	< 0.0	< 0.0
Dilution Factor of stock suspension for the standard ($Dil.F_{RM}$)	1.4	1.1	2.2
Particle size for the sample (d_{NP})	43.9	55.2	16.0
Au mass fraction of the sample (C_S)	18.6	15.8	28.5
Density of the particles (ρ)	< 0.0	< 0.0	< 0.0
Residual	0.5	0.7	0.3
Combined standard uncertainty (%)	10.9 %	10.7 %	6.5 %
Expanded k=2 uncertainty (%)	N/A	21.4 %	13.1 %

For 100 nm AuNPs:	TEM (Supplier) (PNC_{direct}/PNC_{mean}) 120.2 %	HR-SEM (PNC_{direct}/PNC_{mean}) 99.4 %	spICP-MS (PNC_{direct}/PNC_{mean}) 97.2 %
Source of uncertainty	**Relative contribution (%)**	**Relative contribution (%)**	**Relative contribution (%)**
Particle size consensus value for standard ($d_{\mathrm{NP\ RM}}$)	1.7	1.7	2.2
Dilution Factor of stock suspension for the sample ($Dil.F$)	2.8	2.8	3.5
Measurement repeatability (Rep)	2.6	2.6	3.4
Number of observed events for the sample (N_{NP})	18.1	15.7	19.8
Au mass fraction of the standard ($C_{S\ RM}$)	0.3	0.3	0.4
Sample uptake rate for the standard ($q_{liq\ RM}$)	0.2	0.2	0.3
Time of acquisition for the standard ($t_{aq\ RM}$)	< 0.0	< 0.0	< 0.0
Number of observed events for the standard ($N_{NP\ RM}$)	8.5	8.7	11.1
Sample uptake rate for the sample (q_{liq})	0.2	0.2	0.3
Time of acquisition for the sample (t_{aq})	< 0.0	< 0.0	< 0.0
Dilution Factor of stock suspension for the standard ($Dil.F_{RM}$)	3.3	3.4	4.3
Particle size for the sample (d_{NP})	41.2	43.9	28.0
Au mass fraction of the sample (C_S)	20.7	20.2	26.4
Density of the particles (ρ)	< 0.0	< 0.0	< 0.0
Residual	0.4	0.4	0.2
Combined standard uncertainty (%)	11.4 %	9.7 %	7.9 %
Expanded k=2 uncertainty (%)	N/A	19.3 %	15.9 %

Table S-22. Average uncertainty budget for the calculation of $PNC_{distribution}$ of 30 nm, 60 nm, and 100 nm commercial AuNPs, respectively. Full particle size distribution reported by TEM (supplier)16 (first column), HR-SEM[1] (second column), and spICP-MS[1] (third column) were combined with in-house Au mass fraction to derive $PNC_{distribution}$.

For 30 nm AuNPs:	**TEM (Supplier) ($PNC_{distribution}$ 2.14 x 10^{14} L^{-1})**	**HR-SEM ($PNC_{distribution}$ 2.54 x 10^{14} L^{-1})**	**spICP-MS ($PNC_{distribution}$ 2.60 x 10^{14} L^{-1})**
Source of uncertainty	**Relative contribution (%)**	**Relative contribution (%)**	**Relative contribution (%)**
Au mass fraction of the material (C_S)	33.7	6.1	50.3
Particle size for the material (d_{NP})	56.2	91.2	35.3
Density of the particles (ρ)	< 0.0	< 0.0	< 0.0
Spread of particle size distribution	9.8	0.3	14.3
Residual	0.2	2.4	0.1
Combined standard uncertainty (L^{-1})	1.6 x 10^{13} L^{-1}	4.3 x 10^{13} L^{-1}	1.6 x 10^{13} L^{-1}
Expanded k=2 uncertainty (L^{-1})	3.2 x 10^{13} L^{-1}	8.6 x 10^{13} L^{-1}	3.1 x 10^{13} L^{-1}

For 60 nm AuNPs:	**TEM (Supplier) ($PNC_{distribution}$ 2.80 x 10^{13}·L^{-1})**	**HR-SEM ($PNC_{distribution}$ 3.31 x 10^{13} L^{-1})**	**spICP-MS ($PNC_{distribution}$ 3.41 x 10^{13} L^{-1})**
Source of uncertainty	**Relative contribution (%)**	**Relative contribution (%)**	**Relative contribution (%)**
Au mass fraction of the material (C_S)	21.1	18.7	43.3
Particle size for the material (d_{NP})	66.9	77.8	52.8
Density of the particles (ρ)	< 0.0	< 0.0	< 0.0
Spread of particle size distribution	11.6	0.8	3.7
Residual	0.4	2.7	0.2
Combined standard uncertainty (L^{-1})	2.8 x 10^{12} L^{-1}	3.6 x 10^{12} L^{-1}	2.1 x 10^{12} L^{-1}
Expanded k=2 uncertainty (L^{-1})	5.7 x 10^{12} L^{-1}	7.2 x 10^{12} L^{-1}	4.1 x 10^{12} L^{-1}

For 100 nm AuNPs:	**TEM (Supplier) ($PNC_{distribution}$ 5.09 x 10^{12} L^{-1})**	**HR-SEM ($PNC_{distribution}$ 6.27 x 10^{12} L^{-1})**	**spICP-MS ($PNC_{distribution}$ 6.66 x 10^{12} L^{-1})**
Source of uncertainty	**Relative contribution (%)**	**Relative contribution (%)**	**Relative contribution (%)**
Au mass fraction of the material (C_S)	31.4	29.8	46.1
Particle size for the material (d_{NP})	55.8	69.3	51.3
Density of the particles (ρ)	< 0.0	< 0.0	< 0.0
Spread of particle size distribution	12.5	0.4	2.4
Residual	0.4	0.4	0.2
Combined standard uncertainty (L^{-1})	4.9 x 10^{11} L^{-1}	0.5 x 10^{12} L^{-1}	4.6 x 10^{11} L^{-1}
Expanded k=2 uncertainty (L^{-1})	9.7 x 10^{11} L^{-1}	1.0 x 10^{12} L^{-1}	9.2 x 10^{11} L^{-1}

Table S-23. Average uncertainty budget for the ratio between *PNC_{direct}* and *$PNC_{distribution}$*, expressed in percentage, for 30 nm, 60 nm, and 100 nm commercial AuNPs, respectively. *$PNC_{distribution}$* values were derived based on the combination of in-house Au mass fraction and the full size distribution of particle diameters reported by TEM (supplier)[16] (first column), HR-SEM[1] (second column), and spICP-MS[1] (third column).

For 30 nm AuNPs:	**TEM (Supplier)** ($PNC_{direct}/PNC_{distribution}$) **101.5 %**	**HR-SEM** ($PNC_{direct}/PNC_{distribution}$) **83.7 %**	**spICP-MS** ($PNC_{direct}/PNC_{distribution}$) **82.0 %**
Source of uncertainty	**Relative contribution (%)**	**Relative contribution (%)**	**Relative contribution (%)**
Particle size consensus value for standard ($d_{NP\ RM}$)	2.3	0.7	2.8
Dilution Factor of stock suspension for the sample (*Dil.F*)	5.4	2.0	6.6
Measurement repeatability (*Rep*)	3.6	1.1	4.4
Number of observed events for the sample (N_{NP})	19.1	6.0	24.2
Au mass fraction of the standard ($C_{S\ RM}$)	0.5	0.1	0.6
Sample uptake rate for the standard ($q_{liq\ RM}$)	0.3	0.1	0.4
Time of acquisition for the standard ($t_{aq\ RM}$)	< 0.0	< 0.0	< 0.0
Number of observed events for the standard ($N_{NP\ RM}$)	10.2	3.3	12.1
Sample uptake rate for the sample (q_{liq})	0.3	0.1	0.4
Time of acquisition for the sample (t_{aq})	< 0.0	< 0.0	< 0.0
Dilution Factor of stock suspension for the standard ($Dil.F_{RM}$)	2.6	0.9	3.2
Particle size for the sample (d_{NP})	28.3	77.9	13.8
Au mass fraction of the sample (C_S)	21.5	5.4	25.6
Density of the particles (ρ)	< 0.0	< 0.0	< 0.0
Spread of the particle size distribution	5.7	0.2	5.9
Residual	0.2	2.1	0.2
Combined standard uncertainty (%)	9.2 %	14.9 %	6.6 %
Expanded k=2 uncertainty (%)	N/A	29.8 %	13.2 %

For 60 nm AuNPs:	TEM (Supplier) ($PNC_{direct}/PNC_{distribution}$) 101.5 %	HR-SEM ($PNC_{direct}/PNC_{distribution}$) 82.4 %	spICP-MS ($PNC_{direct}/PNC_{distribution}$) 79.7 %
Source of uncertainty	**Relative contribution (%)**	**Relative contribution (%)**	**Relative contribution (%)**
Particle size consensus value for standard ($d_{\mathrm{NP\ RM}}$)	1.3	1.1	2.4
Dilution Factor of stock suspension for the sample ($Dil.F$)	0.6	0.5	0.9
Measurement repeatability (Rep)	2.0	1.8	3.7
Number of observed events for the sample (N_{NP})	8.9	7.5	14.2
Au mass fraction of the standard ($C_{S\ RM}$)	0.3	0.2	0.5
Sample uptake rate for the standard ($q_{liq\ RM}$)	0.2	0.2	0.3
Time of acquisition for the standard ($t_{aq\ RM}$)	< 0.0	< 0.0	< 0.0
Number of observed events for the standard ($N_{NP\ RM}$)	17.9	14.5	29.6
Sample uptake rate for the sample (q_{liq})	0.2	0.2	0.3
Time of acquisition for the sample (t_{aq})	< 0.0	< 0.0	< 0.0
Dilution Factor of stock suspension for the standard ($Dil.F_{RM}$)	1.2	1.1	2.2
Particle size for the sample (d_{NP})	42.6	54.6	16.3
Au mass fraction of the sample (C_S)	17.5	15.8	28.4
Density of the particles (ρ)	< 0.0	< 0.0	< 0.0
Spread of the particle size distribution	7.6	1.9	0.9
Residual	0.5	0.7	0.3
Combined standard uncertainty (%)	10.5 %	7.8 %	5.7 %
Expanded k=2 uncertainty (%)	N/A	17.9 %	11.4 %

For 100 nm AuNPs:	TEM (Supplier) ($PNC_{direct}/PNC_{distribution}$) 106.4 %	HR-SEM ($PNC_{direct}/PNC_{distribution}$) 87.0 %	spICP-MS ($PNC_{direct}/PNC_{distribution}$) 81.5 %
Source of uncertainty	**Relative contribution (%)**	**Relative contribution (%)**	**Relative contribution (%)**
Particle size consensus value for standard ($d_{\mathrm{NP\ RM}}$)	1.4	1.7	2.1
Dilution Factor of stock suspension for the sample (*Dil.F*)	2.3	2.8	3.5
Measurement repeatability (*Rep*)	2.2	2.6	3.3
Number of observed events for the sample (N_{NP})	16.4	15.6	19.1
Au mass fraction of the standard ($C_{S\ RM}$)	0.3	0.3	0.4
Sample uptake rate for the standard ($q_{liq\ RM}$)	0.2	0.2	0.3
Time of acquisition for the standard ($t_{aq\ RM}$)	< 0.0	< 0.0	< 0.0
Number of observed events for the standard ($N_{NP\ RM}$)	7.0	8.6	10.8
Sample uptake rate for the sample (q_{liq})	0.2	0.2	0.3
Time of acquisition for the sample (t_{aq})	< 0.0	< 0.0	< 0.0
Dilution Factor of stock suspension for the standard ($Dil.F_{RM}$)	2.7	3.3	4.2
Particle size for the sample (d_{NP})	38.0	43.9	28.0
Au mass fraction of the sample (C_S)	20.1	20.0	26.5
Density of the particles (ρ)	< 0.0	< 0.0	< 0.0
Spread of the particle size distribution	9.0	0.3	1.2
Residual	0.3	0.4	0.2
Combined standard uncertainty (%)	11.2 %	8.3 %	6.8 %
Expanded k=2 uncertainty (%)	N/A	16.6 %	13.3 %

Table S-24. PNC derived for different commercial AuNPs using in-house Au mass fraction determinations and: the Huber estimates of particle size location (or central tendency) (first column), and the full particle size distribution (second column) measured by spICP-MS.

	Central Tendency (PNC_{mean})[a]	Full PSD ($PNC_{distribution}$)
30 nm PVP		
spICP-MS[b]	$2.06 \times 10^{14} \pm 0.27 \times 10^{14} L^{-1}$	$2.37 \times 10^{14} \pm 0.33 \times 10^{14} L^{-1}$
30 nm bPEI		
spICP-MS[b]	$1.97 \times 10^{14} \pm 0.28 \times 10^{14} L^{-1}$	$2.23 \times 10^{14} \pm 0.34 \times 10^{14} L^{-1}$
30 nm PEG		
spICP-MS[b]	$1.88 \times 10^{14} \pm 0.18 \times 10^{14} L^{-1}$	$2.31 \times 10^{14} \pm 0.24 \times 10^{14} L^{-1}$
60 nm PVP		
spICP-MS[b]	$2.63 \times 10^{13} \pm 0.37 \times 10^{13} L^{-1}$	$3.24 \times 10^{13} \pm 0.47 \times 10^{13} L^{-1}$
60 nm bPEI first lot		
spICP-MS[b]	$2.65 \times 10^{13} \pm 0.55 \times 10^{13} L^{-1}$	$3.18 \times 10^{13} \pm 0.66 \times 10^{13} L^{-1}$
60 nm bPEI second lot		
spICP-MS[b]	$2.87 \times 10^{13} \pm 0.17 \times 10^{13} L^{-1}$	$3.36 \times 10^{13} \pm 0.20 \times 10^{13} L^{-1}$
60 nm PEG first lot		
spICP-MS[b]	$3.42 \times 10^{13} \pm 0.18 \times 10^{13} L^{-1}$	$3.70 \times 10^{13} \pm 0.21 \times 10^{13} L^{-1}$
60 nm PEG second lot		
spICP-MS[b]	$2.56 \times 10^{13} \pm 0.39 \times 10^{13} L^{-1}$	$2.88 \times 10^{13} \pm 0.44 \times 10^{13} L^{-1}$
100 nm Citrate		
spICP-MS[b]	$6.25 \times 10^{12} \pm 0.79 \times 10^{12} L^{-1}$	$7.45 \times 10^{12} \pm 0.95 \times 10^{12} L^{-1}$
100 nm PVP		
spICP-MS[b]	$4.87 \times 10^{12} \pm 0.60 \times 10^{12} L^{-1}$	$5.57 \times 10^{12} \pm 0.70 \times 10^{12} L^{-1}$
100 nm bPEI		
spICP-MS[b]	$4.86 \times 10^{12} \pm 0.86 \times 10^{12} L^{-1}$	$5.39 \times 10^{12} \pm 0.95 \times 10^{12} L^{-1}$

100 nm PEG

spICP-MS[b]	$5.89 \times 10^{12} \pm 1.07 \times 10^{12} L^{-1}$	$6.86 \times 10^{12} \pm 1.25 \times 10^{12} L^{-1}$

[a] Assumes all analyte is present as spherical NPs of the central tendency diameter.

[b] Expanded uncertainties associated with the spICP-MS size determinations included a best estimate of known or suspected sources of bias. Listed uncertainties are based on a confidence interval, with the coverage factor, k = 2 corresponding to approximately 95 % confidence.

Table S-25. Average uncertainty budget for the calculation of PNC_{mean} of 30 nm, 60 nm, and 100 nm commercial AuNPs derived based on the combination of in-house Au mass fraction determinations and the Huber estimates of particle size (or central tendency) results simultaneously obtained by spICP-MS in this study.

For 30 nm AuNPs:	**spICP-MS simultaneous (PNC_{mean} 1.97 x 10^{14} L^{-1})**
Source of uncertainty	**Relative contribution (%)**
Au mass fraction of the material (C_S)	44.1
Particle size for the material (d_{NP})	55.7
Density of the particles (ρ)	< 0.0
Residual	0.2
Combined standard uncertainty (L^{-1})	1.2 x 10^{13} L^{-1}
Expanded k=2 uncertainty (L^{-1})	2.4 x 10^{13} L^{-1}

For 60 nm AuNPs:	**spICP-MS simultaneous (PNC_{mean} 2.83 x 10^{13} L^{-1})**
Source of uncertainty	**Relative contribution (%)**
Au mass fraction of the material (C_S)	44.7
Particle size for the material (d_{NP})	55.2
Density of the particles (ρ)	< 0.0
Residual	0.2
Combined standard uncertainty (L^{-1})	1.7 x 10^{12} L^{-1}
Expanded k=2 uncertainty (L^{-1})	3.3 x 10^{12} L^{-1}

For 100 nm AuNPs:	**spICP-MS simultaneous (PNC_{mean} 5.47 x 10^{12} L^{-1})**
Source of uncertainty	**Relative contribution (%)**
Au mass fraction of the material (C_S)	46.5
Particle size for the material (d_{NP})	53.2
Density of the particles (ρ)	< 0.0
Residual	0.3
Combined standard uncertainty (L^{-1})	4.2 x 10^{11} L^{-1}
Expanded k=2 uncertainty (L^{-1})	8.3 x 10^{11} L^{-1}

Table S-26. Average uncertainty budget for the calculation of *$PNC_{distribution}$* of 30 nm, 60 nm, and 100 nm commercial AuNPs derived based on the combination of in-house Au mass fraction determinations and the full particle size distribution simultaneously obtained by spICP-MS in this study.

	30 nm AuNPs (*$PNC_{distribution}$* 2.30 x 10^{14} L^{-1})	**60 nm AuNPs (*$PNC_{distribution}$* 3.27 x 10^{13} L^{-1})**	**100 nm AuNPs (*$PNC_{distribution}$* 6.32 x 10^{12} L^{-1})**
Source of uncertainty	**Relative contribution (%)**	**Relative contribution (%)**	**Relative contribution (%)**
Au mass fraction of the material (C_S)	41.4	43.6	46.0
Particle size for the material (d_{NP})	51.6	53.6	52.5
Density of the particles (ρ)	< 0.0	< 0.0	< 0.0
Spread of particle size distribution	6.8	2.6	1.3
Residual	0.2	0.2	0.3
Combined standard uncertainty (L^{-1})	0.6 x 10^{13} L^{-1}	0.4 x 10^{12} L^{-1}	0.7 x 10^{11} L^{-1}
Expanded k=2 uncertainty (L^{-1})	3.0 x 10^{13} L^{-1}	4.0 x 10^{12} L^{-1}	9.7 x 10^{11} L^{-1}

Table S-27. Average uncertainty budget for the ratio between PNC_{direct} and PNC_{mean}, expressed in percentage, for 30 nm, 60 nm, and 100 nm commercial AuNPs, respectively. PNC_{mean} values reported for purposes of comparison to PNC_{direct} were derived based on the combination of in-house Au mass fraction and the Huber estimates of particle size (or central tendency) results simultaneously obtained by spICP-MS in this study.

Using spICP-MS simultaneous central tendency:	**For 30 nm AuNPs (PNC_{direct}/PNC_{mean}) 108.0 %**	**For 60 nm AuNPs (PNC_{direct}/PNC_{mean}) 96.7 %**	**For 100 nm AuNPs (PNC_{direct}/PNC_{mean}) 99.3 %**
Source of uncertainty	**Relative contribution (%)**	**Relative contribution (%)**	**Relative contribution (%)**
Particle size consensus value for standard ($d_{NP\ RM}$)	11.1	2.4	1.8
Dilution Factor of stock suspension for the sample ($Dil.F$)	5.2	0.9	3.1
Measurement repeatability (Rep)	3.9	3.8	2.8
Number of observed events for the sample (N_{NP})	9.3	15.0	19.7
Au mass fraction of the standard ($C_{S\ RM}$)	0.4	0.5	0.4
Sample uptake rate for the standard ($q_{liq\ RM}$)	0.3	0.3	0.2
Time of acquisition for the standard ($t_{aq\ RM}$)	< 0.0	< 0.0	< 0.0
Number of observed events for the standard ($N_{NP\ RM}$)	18.5	29.8	9.3
Sample uptake rate for the sample (q_{liq})	0.3	0.3	0.2
Time of acquisition for the sample (t_{aq})	< 0.0	< 0.0	< 0.0
Dilution Factor of stock suspension for the standard ($Dil.F_{RM}$)	2.5	2.3	3.6
Particle size for the sample (d_{NP})	20.9	16.0	32.1
Au mass fraction of the sample (C_S)	27.2	28.4	26.4
Density of the particles (ρ)	0.1	< 0.0	0.1
Residual	0.2	0.3	0.3
Combined standard uncertainty (%)	8.7 %	7.0 %	9.0 %
Expanded k=2 uncertainty (%)	17.4 %	14.0 %	17.9 %

Table S-28. Average uncertainty budget for the ratio between PNC_{direct} and $PNC_{distribution}$, expressed in percentage, for 30 nm, 60 nm, and 100 nm commercial AuNPs, respectively. $PNC_{distribution}$ values reported for purposes of comparison to PNC_{direct} were derived based on the combination of in-house Au mass fraction and the full particle size distribution simultaneously obtained by spICP-MS in this study.

Using spICP-MS simultaneous central tendency:	**For 30 nm AuNPs** ($PNC_{direct}/PNC_{distribution}$) **92.3 %**	**For 60 nm AuNPs** ($PNC_{direct}/PNC_{distribution}$) **83.4 %**	**For 100 nm AuNPs** ($PNC_{direct}/PNC_{distribution}$) **86.2 %**
Source of uncertainty	**Relative contribution (%)**	**Relative contribution (%)**	**Relative contribution (%)**
Particle size consensus value for standard ($d_{NP\ RM}$)	2.6	2.4	1.8
Dilution Factor of stock suspension for the sample (*Dil.F*)	5.6	0.9	3.1
Measurement repeatability (*Rep*)	4.1	3.7	2.8
Number of observed events for the sample (N_{NP})	22.4	14.8	19.4
Au mass fraction of the standard ($C_{S\ RM}$)	0.5	0.5	0.4
Sample uptake rate for the standard ($q_{liq\ RM}$)	0.4	0.3	0.2
Time of acquisition for the standard ($t_{aq\ RM}$)	< 0.0	< 0.0	< 0.0
Number of observed events for the standard ($N_{NP\ RM}$)	11.6	29.3	9.2
Sample uptake rate for the sample (q_{liq})	0.4	0.3	0.2
Time of acquisition for the sample (t_{aq})	< 0.0	< 0.0	< 0.0
Dilution Factor of stock suspension for the standard ($Dil.F_{RM}$)	2.8	2.2	3.5
Particle size for the sample (d_{NP})	22.1	16.1	32.1
Au mass fraction of the sample (C_S)	24.2	28.2	26.3
Density of the particles (ρ)	0.1	< 0.0	< 0.0
Residual	3.1	0.9	0.6
Combined standard uncertainty (%)	0.2	0.2	0.3
Expanded k=2 uncertainty (%)	7.7 %	6.0 %	7.7 %

FIGURES

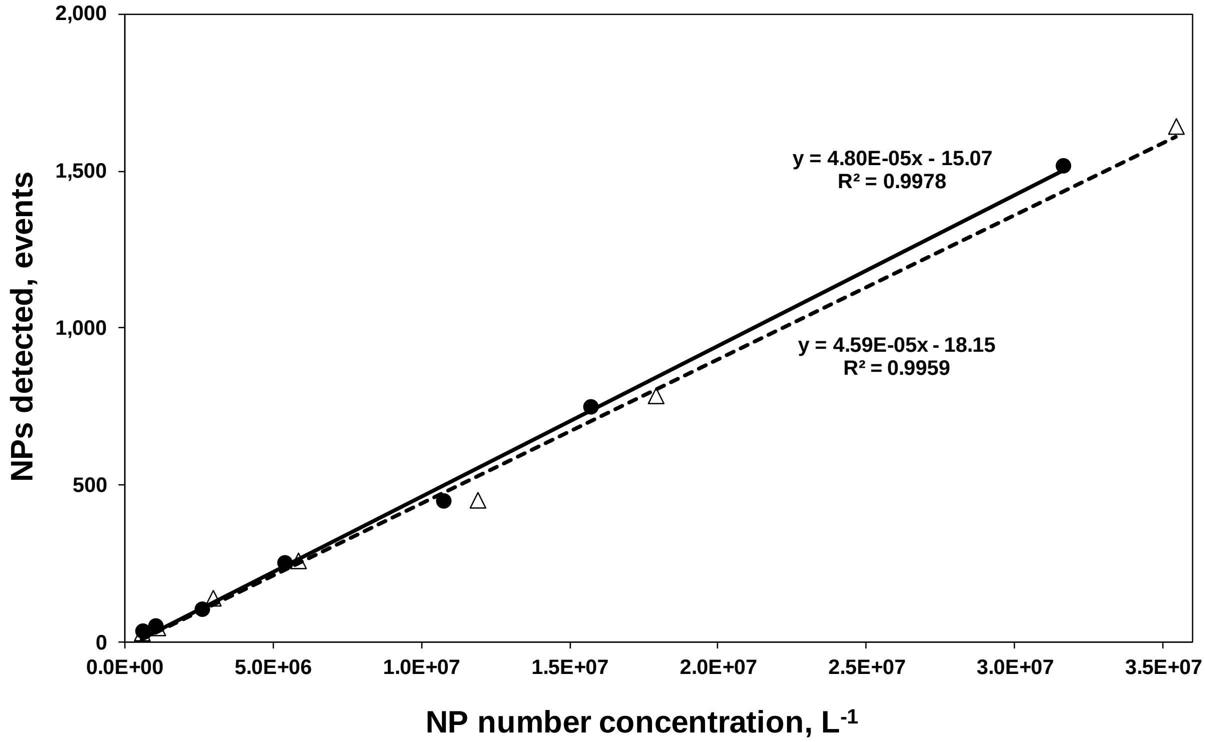

Figure S-1. Particle number concentration *versus* number of events for NIST RM 8012 (△) and NIST RM 8013(•). Solid lines represent the corresponding fit functions after linear regression for RM 8012 (dashed line) and RM 8013 (solid line).

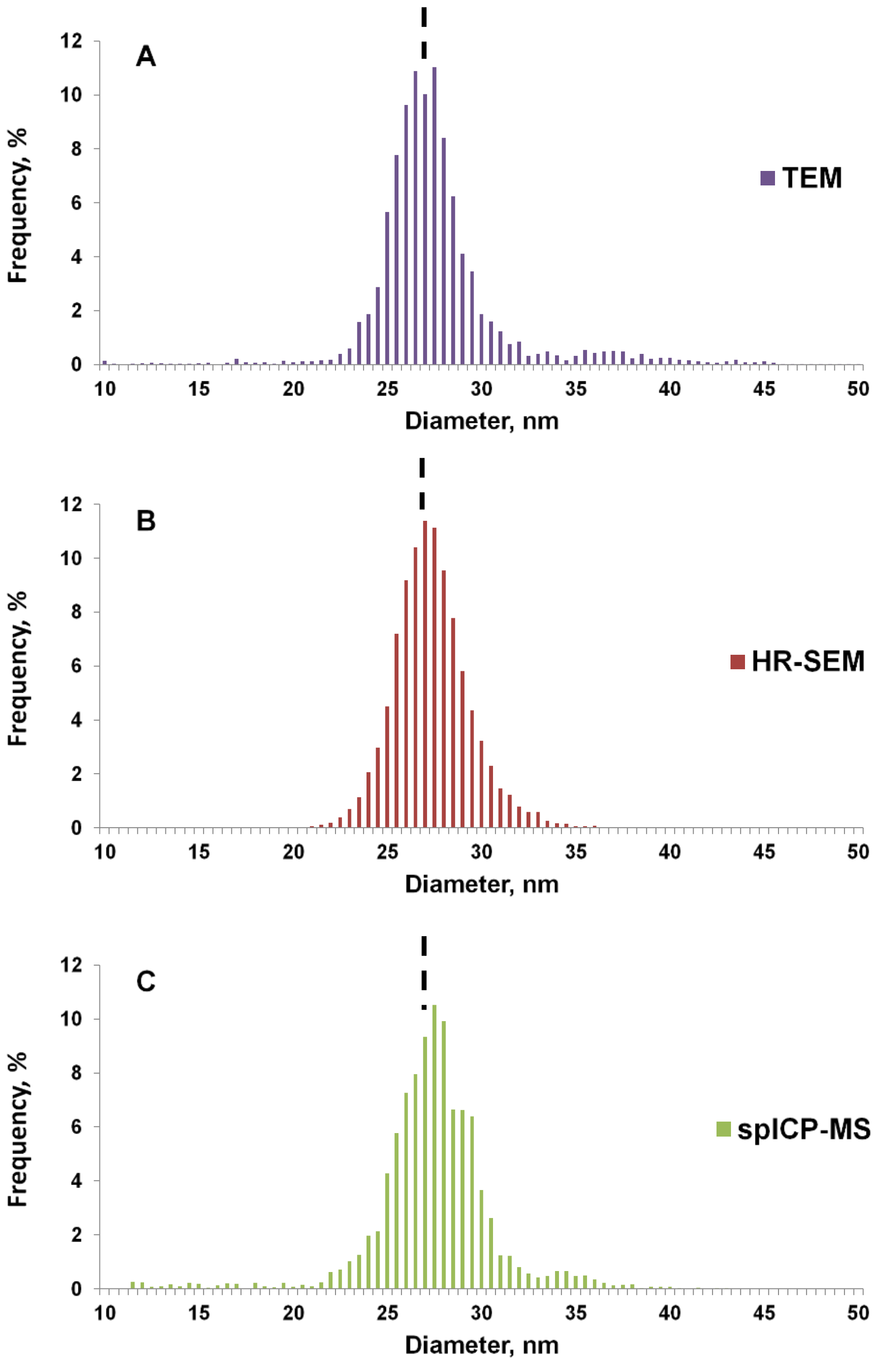

Figure S-2. Reference number size distribution histograms for NIST AuNP RM 8012 reported by (A) TEM (provided in NIST Report of Investigation),[2] (B) HR-SEM,[1] and (C) spICP-MS.[1] Bin size is 0.5 nm. Adapted from ref 1. Vertical black dashed lines indicate mean particle diameters, based on Huber estimates of particle size location (or central tendency).

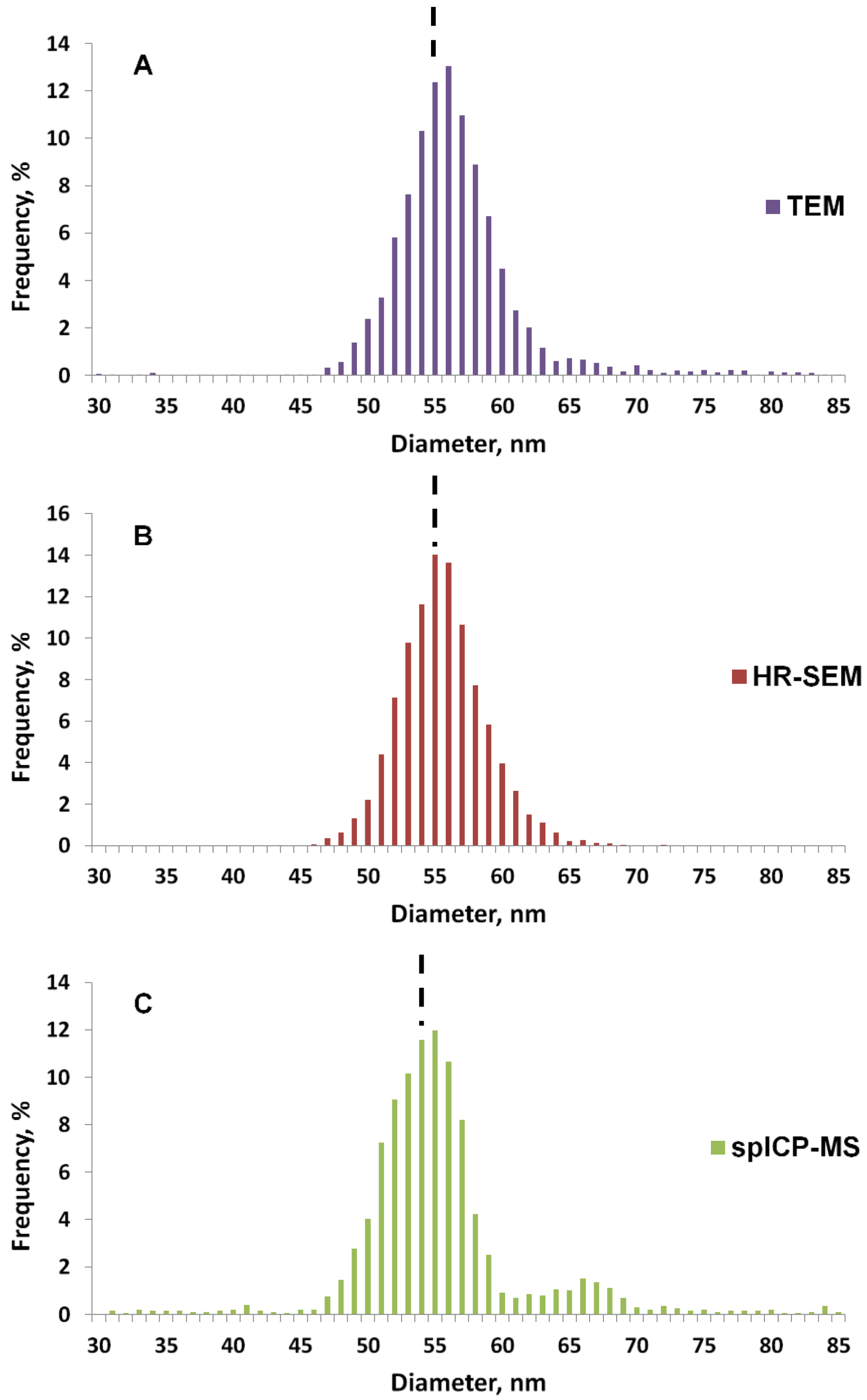

Figure S-3. Reference number size distribution histograms for NIST AuNP RM 8013 reported by (A) TEM (provided in NIST Report of Investigation),[3] (B) HR-SEM,[1] and (C) spICP-MS.[1] Bin size is 0.5 nm. Adapted from ref 1. Vertical black dashed lines indicate mean particle diameters, based on Huber estimates of particle size location (or central tendency).

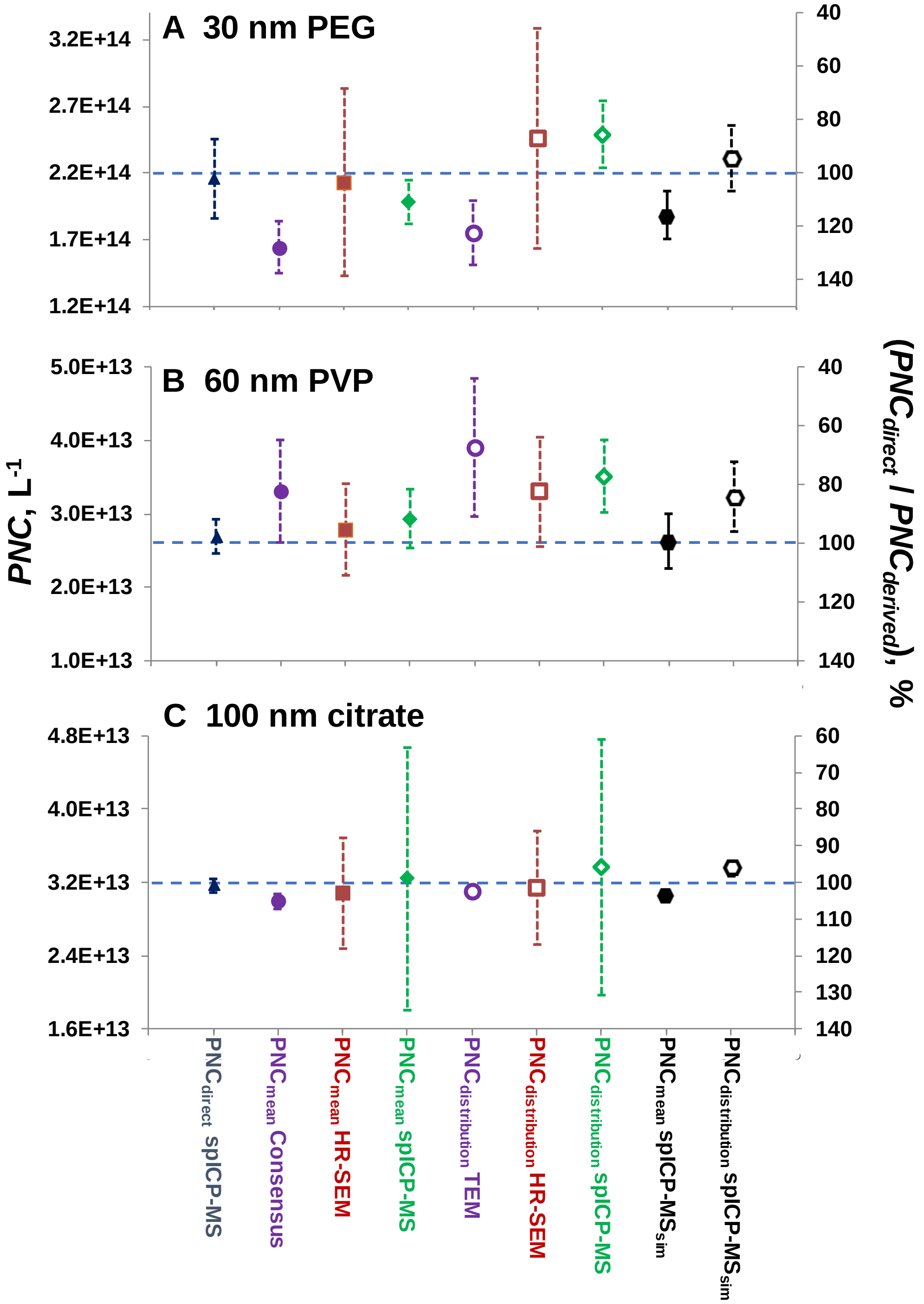

Figure S-4. Comparison for the PNC results (left axis) (*PNC*$_{direct}$ (blue triangles), (*PNC*$_{mean}$ (solid symbols), or *PNC*$_{distribution}$ (open symbols)) and ratio between *PNC*$_{direct}$ and derived PNCs, expressed in percentage, (right axis) for commercial PEG-coated 30 nm AuNPs (A), PVP-coated

60 nm AuNPs, (B), and citrate-coated 100 nm AuNPs (C). Values are provided for spICP-MS (blue triangles for direct PNC measurements, and black hexagons for derived PNC using simultaneous size determinations), TEM (provided by the manufacturer) (purple circles),[16] HR-SEM (dark red squares),[1] and previously reported spICP-MS (green diamonds).[1] The vertical bars indicate *U*95% C.I. for the measured and derived PNC values. Error bars that are not visible are smaller than data points. The horizontal blue lines represent the same value for PNC_{direct} and derived *PNC*.

REFERENCES

(1) Montoro Bustos, A.R., Purushotham, K.P., Possolo, A., Farkas, N., Vladár, A.E., Murphy, K.E., Winchester, M.R. *Anal. Chem.* **2018,** *90,* 14376−14386.

(2) NIST, Reference Material® 8012 Gold Nanoparticles, Nominal 30 nm Diameter; *National Institute of Standards and Technology,* **2015**.

(3) NIST, Reference Material® 8013 Gold Nanoparticles, Nominal 60 nm Diameter; *National Institute of Standards and Technology,* **2015**.

(4) Koepke, A., Lafarge, T., Possolo, A., Toman, B. *NIST Consensus Builder-User's Manual* **2017,** https://consensus.nist.gov/NISTConsensusBuilder-UserManual.pdf.

(5) Koepke, A., Lafarge, T., Possolo, A., Toman, B. *Metrologia* **2017,** *54,* 34-62.

(6) Pace, H.E.; Rogers, N.J.; Jarolimek, C.; Coleman, V.A.; Higgins, C.P.; Ranville, J.F. *Anal. Chem.* **2011**, *83,* 9361−9369.

(7) Degueldre, C.; Favarger, P.Y.; Wold, S. *Anal. Chim. Acta,* **2006,** *555,* 263-268.

(8) Laborda, F., Jimenez-Lamana, J.; Bolea, E.; Castillo, J.R. *J. Anal. At. Spectrom.,* **2013,** *28,* 1220-1232.

(9) Currie, L. A. *Anal. Chem.,* **1968,** *40,* 586-593.

(10) Laborda, F., Jimenez-Lamana, J.; Bolea, E.; Castillo, J.R. *J. Anal. At. Spectrom.,* **2011,** *26,* 1362-1371.

(11) Lin, F. H., Miyashita, S., Inagaki, K., Liu, Y. H., Hsu, I. H. *J. Anal. At. Spectrom.,* **2019,** *34,* 401-406.

(12) Cuello-Nunez, S., Abad-Alvaro, I.; Bartczak, D.; del Castillo Busto, M. E., Alexander Ramsay, D.; Pellegrino, F.; Goenaga-Infante, H. *J. Anal. At. Spectrom.,* **2020,** *35,* 1832-1839.

(13) Beauchamp, C.R., Camara, J.E., Carney, J., Choquette, S.J., Cole, K.D., DeRose, P.C., Duewer, D.L., Epstein, M.S., Polakoski, M., Possolo, A., Sharpless, K.E., Sieber, J.R., Toman, B., Winchester, M.R., Windover, D. *Special Publication (NIST SP) - 260-136,* 2020.

(14) Ramkorun-Schmidt, B., Pergantis, S.A., Esteban-Fernandez, D., Jakubowski, N., Gunther, D. *Anal. Chem.* **2015,** *87,* 8687−8694.

(15) Liu, J., Murphy, K.E., MacCuspie, R.I., Winchester, M.R. *Anal. Chem.* **2014,** *86,* 3405-3414.

(16) Personal communication with the commercial AuNPs supplier company.

(17) *CRC Handbook of Chemistry and Physics;* 88th ed.; Lide, D.R., Ed.; CRC Press: Boca Raton, FL, 2007.